공학석사학위논문

Removal and recovery of copper ions from aqueous solution using magnetic oxidized mesoporous carbon

자성 산화 메조포러스 카본을 이용한

수중 구리 이온의 제거 및 회수

2016 년 2 월

서울대학교 대학원

생태조경·지역시스템공학부

지역시스템공학전공

이 인 걸

Removal and recovery of copper ions from aqueous solution using magnetic oxidized mesoporous carbon

자성 산화 메조포러스 카본을 이용한

수중 구리 이온의 제거 및 회수

지도교수 김 성 배

이 논문을 공학석사 학위논문으로 제출함

2015 년 12 월

서울대학교 대학원
생태조경·지역시스템공학부 지역시스템공학전공

이 인 걸

이 인 걸의 공학석사 학위논문을 인준함

2016 년 1 월

위 원 장 _____ (인)

부위원장 _____ (인)

위 원 _____ (인)

Removal and recovery of copper ions from aqueous solution using magnetic oxidized mesoporous carbon

A THESIS

SUBMITTED TO THE DEPARTMENT OF LANDSCAPE ARCHITECTURE AND RURAL SYSTEMS ENGINEERING

AND THE COMMITEE ON GRADUATE STUDIES OF SEOUL NAIONAL UNIVERSITY IN PARTIAL FULFILLMENT OF THE REQUIREMENTS FOR THE DEGREE OF

MASTER OF ENGINEERING

By

IN-GEOL YI

FEBRUARY, 2016

I certify that I have read this thesis and that in my opinion it is fully adequate, in scope and quality, as thesis for the degree of Master of Engineering.

_____

Chair of Commitee

I certify that I have read this thesis and that in my opinion it is fully adequate, in scope and quality, as thesis for the degree of Master of Engineering.

_____

Vice-Chair of Commitee

I certify that I have read this thesis and that in my opinion it is fully adequate, in scope and quality, as thesis for the degree of Master of Engineering.

_____

Member

Abstract

The objective of this study was to investigate the copper ions removal and recovery from aqueous solution using magnetic-oxidized-mesoporous carbon as adsorbent. Mesoporous carbon was synthesized by multi-step using mesoporous silica as hard-template. Magnetic-oxidized-mesoporous carbon (M-O-MC) was prepared by nitric acid treatment and co-precipitation with iron oxide. Transmission electron microscope (TEM) images showed that mesoporous carbons had nano-sized mesopores on surface but those pores are decreased by surface functionalization. Energy dispersive x-ray spectrometer (EDS) analysis indicated that oxygen and iron were attached on the surface of mesoporous carbon after surface functionalization. In the N_2 adsorption-desorption analysis, surface functionalization resulted in decrease of BET specific surface area, total pore volume, and mesopore area of mesoporous carbon from 1,488.10 m^2/g, 1.40 m^3/g, 1251.00 m^2/g to 179.19 m^2/g, 0.18 m^3/g, 130.60 m^2/g respectively. From the XRD analysis, maghemite peaks appeared in M-O-MC. FT-IR spectra showed that carboxylic bonds and Fe-O bond were assigned on M-O-MC by surface functionalization.

In order to investigate the adsorption properties of copper ions onto M-O-MC, batch experiments were conducted. The adsorption capacity of copper ions increased from 3.70 mg/g to 34.89 mg/g by surface functionalization. It is considered that carboxyl group contributed to the elevation of copper

adsorption capacity. From the kinetic test data, copper ions adsorption increased as contact time went on, and well fitted by Pseudo-first-order model. Equilibrium test data were well described by Freundlich isotherm model. The maximum adsorption capacity was calculated to be 48.354 mg/g at dose of 1 g/L from Langmuir isotherm model. The adsorption capacity of copper increased at higher temperature than that of at low temperature indicating that reaction between copper ions and M-O-MC was endothermic and spontaneous. In the test for studying the effect of pH and ionic strength on copper ions adsorption, the adsorption capacity decreased at acidic condition and high concentration of salts. It is considered that protons and salt cations competed with copper ions for adsorption sites on M-O-MC. Binary adsorption test for competition with other heavy metals showed that copper ions had stronger affinity with surface of M-O-MC than nickel, zinc, and cobalt ions. Thus, M-O-MC could be applied for selective adsorption of copper ions in aqueous solution containing nickel, zinc, cobalt ions. Copper ions adsorbed on M-O-MC surface were thoroughly desorbed by 0.1 M HCl solution. Using this solvent, M-O-MC was repeatedly used for 4 times. The results showed that the adsorption capacity decreased by half at 2^{nd} cycle and maintained that capacity at 3^{rd} and 4^{th} cycles. Meanwhile, copper ions and iron ions were simultaneously desorbed and leached in the process of desorption. In order to separate and recover copper from aqueous solution containing iron ions, solution pH was

adjusted by 2 M NaOH. At pH 5, iron ions were precipitated firstly, and copper ions were sequentially precipitated at pH above 6. This study demonstrated that M-O-MC could be applied for adsorbents to remove and recover copper ions from aqueous solution.

Keywords: mesoporous carbon, magnetic-oxidized-mesoporous carbon, copper, adsorption, recovery, precipitation

Contents

List of Tables

List of Figures

I. Introduction

1.1 Background

Copper has signature strengths such as high electrical and thermal conductivity, corrosion resistance (Ozer et al., 2003). Therefore, it is one of the most widely used heavy metals from ancient times to these days. Copper has been applied by widespread industries such as semiconductor, electroplating, mining, and so on (Ochoa-Herrera et al., 2011). However, according to U.S. geological survey's research (2010), it was estimated that copper has only 34 years of minable reserves and worried about exhaustion. Meanwhile, Korea is one of the major consumers of copper, but depends heavily on import from abroad (JOGMEC, 2010). Thus, it is necessary to recover the discharged copper from wastewater for recycling.

Meanwhile, copper is toxic for living organisms like other heavy metals. Copper is mainly spilled from mining, smelting, electroplating industries (Boujelben et al., 2009). When it is exposed to environment excessively, it can be accumulated in the organisms and cause liver damage, lung cancer, etc. (Hu et al., 2013) to human beings. Therefore, it is necessary to remove copper from industrial effluents.

There are many technologies to remove copper ions from aqueous solutions including chemical-precipitation (Mirbagheri & Hosseini, 2004), ion-exchange

(Keane, 1998), filtration (Ahmad & Ooi, 2010), adsorption, etc. Among these methods, adsorption is considered as one of the most effective and economic methods (Mi et al., 2012).

Mesoporous carbon is one of the promising novel materials, since it has large specific surface area, high specific pore volume, and good thermal, chemical stabilities (Xin & Song, 2015). For this reason, there have been many researches for application of mesoporous carbon such as catalyst supports (Joo et al., 2006), drug delivery (Zhu et al., 2012), fuel cell (Chang et al., 2007). Also, mesoporous carbon has been investigated as candidates for adsorbents for organic pollutants, dyes, etc. due to its above-mentioned good properties. However, because of its hydrophobicity, it needs to be functionalized for enhancing adsorption property to heavy metals (Baniamerian et al., 2009).

1.2 Objective

The objective of this study is to investigate the copper ions removal and recovery from aqueous solution using magnetic-oxidized-mesoporous carbon as adsorbents.

1.3 Method of approach

The characteristics of magnetic-oxidized-mesoporous carbon were analyzed using Transmission electron microscope (TEM), Field emission scanning electron microscopy (FESEM), Energy Dispersive X-ray Spectrometer (EDS), X-ray diffraction (XRD) spectrometer, Fourier transform infrared (FTIR) spectrometer, Dynamic light scattering (DLS) spectrometer, and nitrogen gas (N_2) adsorption-desorption experiments. Kinetic, equilibrium, and thermodynamic experiments were performed to observe the adsorption characteristics of copper ions onto magnetic-oxidized-mesoporous carbon. The effects of solution composition (pH, ionic strength, other heavy metal) were also studied by batch experiments. Finally, reusability of magnetic-oxidized-mesoporous carbon on copper ions removal was investigated and the adsorbed copper was recovered by precipitation.

II. Literature Review

Several researchers have investigated the removal of heavy metals using mesoporous carbon (Table 2-1). Gu et al. (2007) developed iron-containing ordered mesoporous carbon and studied its application for arsenic adsorption from water. Baniamerian et al. (2009) synthesized chemically oxidized mesoporous carbon to investigate the removal of lead ion from water. Anbia & Amirmahmoodi (2011) impregnated mesoporous carbon with anionic and cationic surfactants to enhance the adsorption capacity of mercury and Manganese. Baikousi et al. (2012) synthesized magnetic Fe_2O_3/mesoporous carbon hybrid and investigated its potential for application in hexavalent chromium ions. Chen et al. (2014) reported copper ions removal using magnetically separable nitrogen-doped mesoporous carbon. Moreno-Tovar et al. (2014) developed oxidized mesoporous carbon and investigated its application for lead and cadmium removal. Barczak et al. (2015) prepared mesoporous carbon, oxidized mesoporous carbon, and amino-functionalized mesoporous carbon, then tested their adsorption capacity of bivalent heavy metal ions (lead, cadmium, zinc, and copper) from aqueous solution.

Although there were some studies reporting copper ions adsorption characteristic by surface-functionalized mesoporous carbon, it needs more studies to investigate the influence factors (ionic strength, other heavy metal)

on copper adsorption by mesoporous carbon. Also, there is little previous research studying copper recovery after adsorption onto mesoporous carbon.

In the present study, not only basic factors like contact time, initial copper concentration, but the effects of solution composition such as ionic strength and other heavy metals in copper adsorption were also examined. Besides, the method for recovering copper was investigated.

Table 2-1. Previous researches for heavy metal removal by mesoporous carbon

Author	Title	Adsorbent	Summary
Gu et al. (2007)	Synthesis and evaluation of iron-containing ordered mesoporous carbon (FeOMC) for arsenic adsorption	Iron-containing ordered mesoporous carbon	An ordered nano-structured adsorbent, iron-containing ordered mesoporous carbon (FeOMC) was developed for arsenic adsorption from water. Arsenic adsorption experiments showed that the maximum arsenic adsorption was primarily controlled by the amount of iron impregnated, and the molar ratio of iron and the maximum amount of arsenate adsorption was 5.53–7.97.
Gu & Deng (2007)	Arsenic sorption and redox transformation on iron-impregnated ordered mesoporous carbon	Iron-impregnated ordered mesoporous carbon	An iron-modified ordered mesoporous carbon (FeOMC) for its ability to adsorb arsenic from the aqueous phase. Batch experiments showed that the pH level of the solution had a major impact on arsenic sorption. Adsorption of arsenic on FeOMC could be well explained by the surface complexation model.
Baniamerian et al. (2009)	The effect of surface modification on heavy metal ion removal from water by carbon nanoporous adsorbent	Chemically oxidized mesoporous carbon	Chemically oxidized mesoporous carbon (COMC) with excellent lead adsorption performance was prepared by an acid surface modification method from mesoporous carbon (MC) by wet impregnation method. The larger adsorption capacity of chemically oxidized mesoporous carbon for Pb(II) is mainly due to the oxygenous functional groups formed on the surface of COMC which can react with Pb(II) to form salt or complex deposited on the surface of MC.

Author	Title	Adsorbent	Summary
Yazdankhah et al. (2010)	Enhanced sorption of cadmium ion on highly ordered nanoporous carbon by using different surfactant modification	Surfactants modified ordered mesoporous carbon	The effect of different type of surfactants on the adsorption of Cd(II) on ordered mesoporous carbon was investigated using cationic, anionic and non-ionic surfactant. The Cd(II) removal for cationic surfactant cetylpyridinium chloride (CPC), non-ionic surfactant Triton X-100 (TX), anionic surfactant sodium dodecyl sulfate (SDS) modified mesoporous carbon and unmodified mesoporous carbons were found to be 94.5%, 88.4%, 84% and 68%, respectively.
Anbia & Amirmahmoodi (2011)	Removal of Hg (II) and Mn (II) from aqueous solution using nanoporous carbon impregnated with surfactants	Surfactants modified mesoporous carbon	Mesoporous carbons were impregnated with the anionic and cationic surfactants to increase adsorbing capacity for heavy metal ions. The mercury removal by cationic surfactant cetyltrimethyl ammonium bromide (CTAB), anionic surfactant sodium dodecyl sulfate (SDS) modified mesoporous carbon and unmodified mesoporous carbon were found to be 94%, 81.6% and 54.5%, respectively while the manganese removal for these adsorbents were found to be 82.2%, 70.5% and 56.8%, respectively.
Chen et al. (2011)	Synthesis of ordered large-pore mesoporous carbon for Cr(VI) adsorption	Highly ordered mesoporous carbon with large accessible pores	Highly ordered mesoporous carbon with large accessible pores (OMC-P) was prepared by using laboratory-made poly(ethylene oxide)-b-polystyrene diblock copolymer as template via the evaporation-induced self-assembly method. The prepared OMC-P exhibits much higher adsorption performance than amphiphilic triblock copolymer F127 templated ordered mesoporous carbon and commercial activated carbon

Author	Title	Adsorbent	Summary
Zolfaghari et al. (2011)	Taguchi optimization approach for Pb(II) and Hg(II) removal from aqueous solutions using modified mesoporous carbon	Zinc oxide-modified mesoporous carbon	Using the Taguchi method, a systematic optimization approach for removal of lead (Pb) and mercury (Hg) by a nanostructure, zinc oxide-modified mesoporous carbon CMK-3 denoted as Zn-OCMK-3 was presented. Under optimum conditions, the pollutant removal efficiency (PRE) was 97.25% for Pb(II) and 99% for Hg(II).
Baikousi et al. (2012)	Synthesis and characterization of γ-Fe2O3 /Carbon hybrids and their application in removal of hexavalent chromium ions from aqueous solutions	Magnetic Fe2O3/mesoporous carbon hybrid	Magnetic Fe2O3/carbon hybrids were prepared in a two-step process. The kinetic studies showed a rapid removal of Cr(VI) ions from the aqueous solutions in the presence of these magnetic mesoporous hybrids and a considerably increased adsorption capacity per unit mass of sorbent in comparison to that of pristine CMK-3 carbon. The results also indicate highly pH-dependent sorption efficiency of the hybrids, whereas their kinetics was described by a pseudo-second-order kinetic model.
Baikousi et al. (2013)	Novel ordered mesoporous carbon with innate functionalities and superior heavy metal uptake	Ordered mesoporous carbons with innate carbonyl functionalities	Ordered mesoporous carbons with innate carbonyl functionalities (MC-icf) have been synthesized via a nanocasting process using SBA-15 as a template and acetylenedicarboxylic acid as a carbon source, instead of the commonly used sugar. Adsorption experiments data indicated an improved and selective capability for Cd2+, Pb2+, and Cu2+ uptake by the MC-icf compared with the standard CMK-3.

Author	Title	Adsorbent	Summary
Huang & He (2013)	Electrosorptive removal of copper ions from wastewater by using ordered mesoporous carbon electrodes	Ordered mesoporous carbon electrodes	Electrosorption performance of copper ions from wastewater on ordered mesoporous carbon (OMC) electrode was investigated. At pH = 4, the saturated adsorption capacity of copper ion (Cu^{2+}) on the OMC electrode was determined 9.53 mg/g at open circuit. The equilibrium electrosorption capacity at polarization of 0.9 V was 56.62 mg/g, which is about 5 times higher than that at open circuit.
Anbia & Dehghan (2014)	Functionalized CMK-3 mesoporous carbon with 2-amino-5-mercapto-1,3,4 -thiadiazole for Hg(II) removal from aqueous media	2-amino-5-mercapto-1,3,4-thiadiazole modified ordered mesoporous carbon	Ordered mesoporous carbon (CMK-3) was synthesized and functionalized with 2-amino-5-mercapto-1,3,4-thiadiazole groups (AMT-OCMK-3) for Hg(II) removal from aqueous solution. The results showed that the enrichment factor for Hg(II) was 250, the precision (relative standard deviation (RSD), %) for six replicate measurements was 2.05% and the limit of detection for Hg(II) was achieved at 0.17 µg/L.
Chen et al. (2014)	Solid–solid grinding/templating route to magnetically separable-nitrogen doped mesoporous carbon for the removal of Cu^{2+}ions	Magnetically separable nitrogen – doped mesoporous carbon	N-doped ordered mesoporous carbon materials (NOMC) with 2D hexagonal symmetry structure were synthesized via a facile solid–solid grinding/templating route, in which the ionic liquids (ILs) of 1-cyanoethyl-3-methylimidazolium chloride and SBA-15 were employed as the precursor and hard template, respectively. Magnetic iron nanoparticles were successfully embedded into the carbon matrix by introducing iron chloride to the mixture of SBA-15 and ILs during the synthesis process. The NOMC-Fe composite possessed superior adsorption capacity of Cu^{2+}ions (23.6 mg/g).

Author	Title	Adsorbent	Summary
Chen et al. (2014)	Adsorption of Cr(VI) from aqueous solution on mesoporous carbon nitride	Mesoporous carbon nitride	Mesoporous carbon nitride (MCN) was synthesized using mesoporous silica SBA-15 as the template and employed for the adsorption of Cr(VI) from aqueous solutions. The maximum sorption capacity of MCN for Cr(VI) was 48.31 mg/g at pH 5.7, higher than activated carbon (AC) and ordered mesoporous carbon (CMK-3).
Moreno-Tovar et al. (2014)	Oxidation and EDX elemental mapping characterization of an ordered mesoporous carbon: Pb(II) and Cd(II) removal	Oxidized mesoporous carbon	The adsorption of the metallic ions Cd(II) and Pb(II) onto the surface of the mesoporous activated carbon CMK-3 is presented. The adsorption isotherms follow the Langmuir model and the maximum amount of adsorbed ions was 40.4 mg/g for Cd(II) and 94 mg/g for Pb(II) at pH 5 and 25 ℃.
Tang et al. (2014)	Synergistic effect of iron doped ordered mesoporous carbon on adsorption-coupled reduction of hexavalent chromium and the relative mechanism study	Iron doped ordered mesoporous carbon	A magnetic iron nanoparticles doped ordered mesoporous carbon (Fe/CMK-3) was successfully prepared for highly effective removal of Cr(VI). Fe/CMK-3 exhibited higher Cr(VI) removal efficiency (97%), broader pH scope of application and easier separation compared with pristine ordered mesoporous carbon (CMK-3). X-ray photoelectron spectroscopy (XPS) analysis demonstrated that the Cr(VI) removal was a adsorption and synergistic reduction process owing to trivalent chromium Cr(III) occurring on the surface of Fe/CMK-3.
Yang et al. (2014)	Effective removal of Cr(VI) through adsorption and reduction by magnetic mesoporous carbon incorporated with polyaniline	Magnetic mesoporous carbon incorporated with polyaniline	Magnetic mesoporous carbon incorporated with polyaniline (PANI–Fe/OMC) is developed for enhanced adsorption and reduction of toxic Cr(VI) to non-toxic Cr(III). The adsorption capacity of the functionalized material is two- and ten-fold that of the magnetic mesoporous carbon (Fe/OMC) and pristine mesoporous silicon (SBA-15), respectively. the amino groups on the surface of PANI–Fe/OMC are involved in Cr(VI) uptake, and simultaneously some toxic Cr(VI) are reduced to non-toxic Cr(III) during the removal process.

Author	Title	Adsorbent	Summary
Anbia & Haqshenas (2015)	Adsorption studies of Pb(II) and Cu(II) ions on mesoporous carbon nitride functionalized with melamine-based dendrimer amine	Mesoporous carbon nitride functionalized with melamine-based dendrimer amine	Mesoporous carbon nitride functionalized with melamine-based dendrimer amine has been developed. The Pb(II) and Cu(II) removal by mesoporous carbon nitride functionalized with melamine based dendrimer amine was found to be 196.34 and 199.75 mg/g, respectively.
Baikousi et al. (2015)	Synthesis and characterization of robust zero valent iron/mesoporous carbon composites and their applications in arsenic removal	Nanoscale zero valent iron/mesoporous carbon composite	Nanoscale zero valent iron particles (nZVI) have been developed by in situ reduction of Fe^{3+} ions onto a mesoporous type of carbon matrix – starch-derived mesoporous carbonaceous material previously reported and marketed commercially as ‘‘Starbon’’. The nZVI/Starbon hybrid has been tested as absorbent for As(III) removal showing a total removal of 358 lmol (26.8 mg) of As(III) per gram of the composite at pH = 7.
Barczak et al. (2015)	Ordered mesoporous carbons as effective sorbents for removal of heavy metal ions	Pristine, oxidized, and amino -functionalized mesoporous carbon	The systematic study on adsorption of heavy metal ions by ordered mesoporous carbon CMK-3. This sorbent has been obtained by hard templating using SBA-15 and subsequently, oxidized (by treatment with (NH4)2S2O8/H2SO4) and amino-functionalized (by treatment with N-(3-trimethoxysilylpropyl) diethylenetriamine). The observed static sorption capacities are very high up to 0.8 mmol/g and were at least twice higher than the values corresponding to the commercial activated carbon Norit® SX2.
Dai et al. (2015)	Carbothermal synthesis of ordered mesoporous carbon-supported nano zero-valent iron with enhanced stability and activity for hexavalent chromium reduction	Nano zero-valent iron and ordered mesoporous carbon composite	Composites of nano zero-valent iron (nZVI) and ordered mesoporous carbon (OMC) are prepared by using simultaneous carbothermal reduction methods. Cr(VI) can be rapidly removed by nZVI/OMC-3, which has high SBET(715.16 m2/g) and small nZVI particle sizes (20–30 nm), which are conducive to the reduction and mass transfer of Cr(VI).

Author	Title	Adsorbent	Summary
Guo et al. (2015)	Synthesis and application of 8-hydroxyquinoline modified magnetic mesoporous carbon for adsorption of multivariate metal ions from aqueous solution	8-hydroxyquinoline modified magnetic mesoporous carbon	The new 8-hydroxyquinoline (8-HQ) modified magnetic mesoporous carbon (8-HQ-Ni-CMK-3) was prepared and applied for adsorption of multivariate metal ions from aqueous solution. The adsorption behaviors of multivariate metal ions in aqueous solution onto the adsorbent were compared with G, 8-HQ-G, and Ni-CMK-3 at the same time. It is found that the maximum adsorption capacity of Cu(II), Pb(II), Sr(II), and Co(II) on 8-HQ-Ni-CMK-3 could reach 2.45 mg/g, 2.35 mg/g, 1.05 mg/g, and 1.14 mg/g in 30 min at pH 5.0, respectively.
Li & Ren (2015)	Preparation of nitrogen-functionalized mesoporous carbon and its application for removal of copper ions	Nitrogen-functionalized mesoporous carbon	Nitrogen-functionalized mesoporous carbon (NMC) materials with high nitrogen content were synthesized through a hard template method using ionic liquid of 1-cyanomethyl-3-methylimidazolium bromide as the precursor and LUDOX HS-40 colloidal silica as the template. The adsorption performance of the prepared NMCs was investigated by removing Cu^{2+} from aqueous solutions and the adsorption capacity could attain 117.1 mg g-1 at an optimal condition.
Lu et al. (2015)	Removal characteristics of Cd(II) ions from aqueous solution on ordered mesoporous carbon	Ordered mesoporous carbon	Ordered mesoporous carbon (CMK-3) was synthesized using SBA-15 mesoporous molecular sieve as a template and sucrose as carbon source. The effect of pH, contact time and temperature on adsorption process was investigated in batch experiments. The results showed that the removal percentage could reach ca. 90% at the conditions of initial Cd(II) ions concentration of 20 mg/L, dose of 20mg, pH 6.5, contact time of 3h and 293K.

Author	Title	Adsorbent	Summary
Yang et al. (2015)	Simultaneous removal of lead and phenol contamination from water by nitrogen-functionalized magnetic ordered mesoporous carbon	Nitrogen-functionalized magnetic ordered mesoporous carbon	A novel nitrogen-functionalized magnetic ordered mesoporous carbon (N-Fe/OMC) with uniform pore size (3.8 nm) and excellent magnetic property (8.46 emu/g) was fabricated through simple impregnation then polymerization and calcination. The resultant adsorbent exhibited more preferential sorption toward Pb(II) and phenol than simple equivalent mixture of magnetic ordered mesoporous carbon (Fe/OMC) and pristine ordered mesoporous carbon (OMC).
Zeng et al. (2015)	Enhancement of Cd(II) adsorption by polyacrylic acid modified magnetic mesoporous carbon	Polyacrylic acid modified magnetic mesoporous carbon	A novel adsorbent was prepared by chelating magnetic mesoporous carbon with polyacrylic acid (PAA) to improve the performance of Cd(II) adsorption. The modification accelerated the cadmium adsorption rate. And equilibrium data were best described by Langmuir model, and the estimated maximum adsorption capacity for the modified adsorbent increased to 406.6 mg/g, which was 140.8% higher than the pristine materials.

III. Materials and Methods

3.1 Synthesis of mesoporous carbon

Prior to synthesize mesoporous carbon, mesoporous silica templates were prepared according to Zhao et al. (1998). At first, 6 g of Pluronic P123 (Sigma Aldrich) and 1 g of cetyltrimethylammonium bromide (CTAB, ≥99%, Sigma Aldrich) were dissolved in a mixed solution of 80 mL of deionized water (Direct-Q, Millipore), 50 mL of ethanol (≥94%, Duksan), and 100 mL of 2 M HCl (37%, Duksan). After stirring at 30 ℃ for 1 hour, 20 mL of tetraethylorthosilicate (TEOS, ≥99%, Sigma Aldrich) was added into the solution, and stirred for 45 minutes at 40 ℃. Then, the solution was aged at 80 ℃ for 24 hours under refluxing condition. The resultants were filtered and washed with deionized water, and dried under ambient conditions. Finally, the dried powder was calcined at 550 ℃ for 6 hours using muffle furnace to remove the surfactant. Schematic diagram for mesoporous silica synthesis is shown in Figure 3-1.

Mesoporous carbon was synthesized according to the process of the literature (Tang et al., 2014). 10 mL of mixed solution containing 2.5 g of sucrose (Wako) and 0.28 g of H_2SO_4 (≥95%, Duksan) was prepared, and 2 g of above-mentioned mesoporous silica templates were added into the solution. The

mixture was heated in an oven at 100 ℃ for 6 hours and 160 ℃ for 6 more hours. To sufficiently fill the inside of pores of mesoporous silica templates by sucrose, pre-treated powders were added into 5 mL of mixed solution containing 1.6 g of sucrose and 0.18 g of H_2SO_4 and heated as mentioned above. The obtained material was calcined in a nitrogen condition at 900 ℃ for 6 hours with a constant heating rate of 5 ℃/min using tube furnace (FT-1230, DAIHAN Scientific). The resultants were boiled in 500 mL of 1 M NaOH (Duksan) solution (50 vol% ethanol-50 vol% H_2O) at 80 ℃ to remove silica templates. Finally, the resultants were filtered and washed with 50 % ethanol until the pH was approached to 7, and dried at 60 ℃ for 24 hours. Thus, mesoporous carbon was synthesized.

3.2 Synthesis of magnetic-oxidized-mesoporous carbon

Before embedding magnetic property to mesoporous carbon, acid treatment was conducted to enhance its copper adsorption capacity and give affinity to iron oxide (Moreno-Tovar et al., 2014). At first, 0.5 g of mesoporous carbon was added into 50 mL of HNO_3 (70%, Daejung) and boiled at 70 ℃ for 12 hours under refluxing condition. Then, the resultants were filtered and washed with deionized water several times to neutralize, and dried at 110 ℃ for 6 hours. Thus, oxidized-mesoporous carbon was obtained**.**

In order to embed magnetic property, 0.2 g of oxidized-mesoporous carbon was added to 400 mL of the mixed solution which contains 0.01 mol of $FeCl_3 \cdot 6H_2O$ (Duksan) and 0.005 mol of $FeSO_4 \cdot 7H_2O$ (Junsei) (Fe(III)/Fe(II) molar ratio = 2). After vigorous stirring for well dispersion, 6 M NaOH was added by drop-wise until the solution pH reached 8.7 and stirred 12 more hours. Then, the precipitates were washed with deionized water and dried at 150 ℃ for 6 hours. Thus, magnetic-oxidized-mesoporous carbon was synthesized. Schematic diagram for magnetic-oxidized-mesoporous carbon synthesis is shown in Figure 3-2.

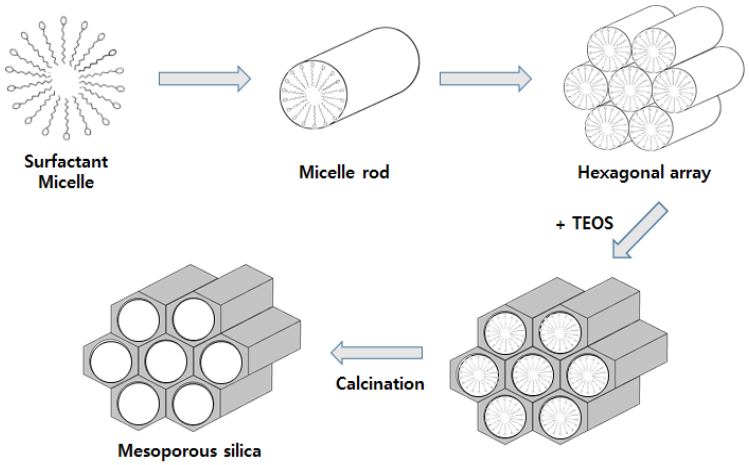

Figure 3-1. Schematic diagram for mesoporous silica synthesis (Zhao et al., 1998)

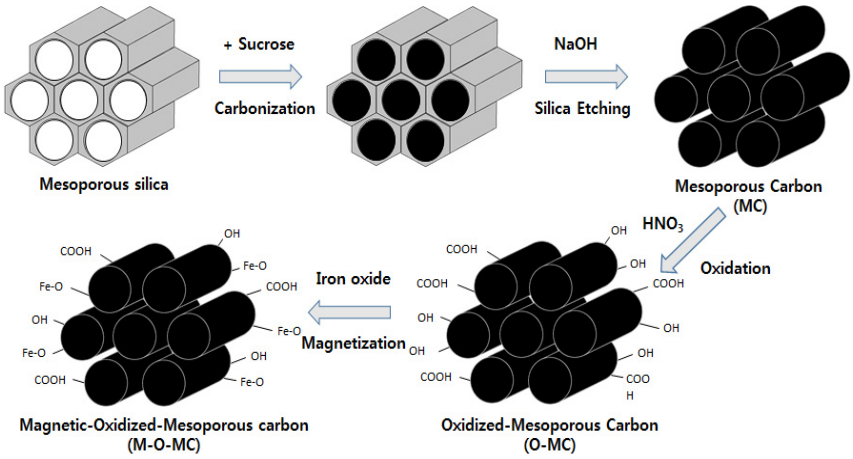

Figure 3-2. Schematic diagram for magnetic-oxidized-mesoporous carbon synthesis (Tang et al., 2014, Moreno-Tovar et al., 2014)

Figure 3-3. Muffle furnace (left) and tube furnace (right)

3.3 Characterization of mesoporous carbon

Field emission scanning electron microscopy (FE-SEM) and energy dispersive x-ray spectrometer (EDS) analysis were performed by field emission scanning electron microscope (SUPRA 55VP, Carl Zeiss, Germany). TEM images were obtained by High resolution-transmission electron microscope (JEM-3010, JEOL, Japan). The crystalline structures were examined by X-ray diffractometry (D8 Advance, Bruker, Germany) with Cu Kα radiation at fixed power source (40 kV and 30 mA). Infrared spectra was obtained using Fourier transform infrared spectrometer (Nicolet 6700, Thermo Scientific, USA) with KBr pellets. Dynamic light scattering spectrophotometer (DLS-7000, Otsuka Electronics, Japan) was used to examine particle size distribution. Nitrogen gas (N_2) adsorption-desorption experiments were performed using a surface area analyzer (BELSORP-mini II, BEL Japan, Japan).

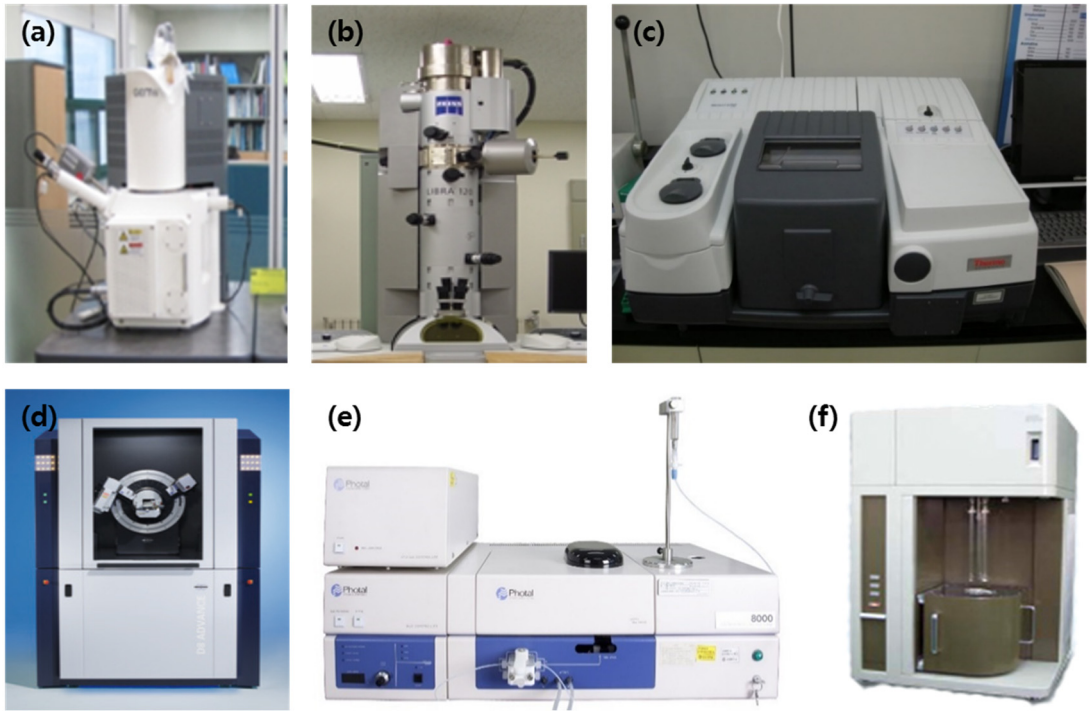

Figure 3-4. Instruments for characterization: (a) FE-SEM, (b) HR-TEM, (c) FT-IR, (d) XRD, (e) DLS, (f) Surface area analyzer

3.4 Batch experiments

3.4.1 Copper adsorption property

The desired copper solutions were prepared by diluting the stock solution made by $CuCl_2 \cdot 2H_2O$ (Duksan). All the batch experiments were conducted in 15 mL of polypropylene conical tubes and solution pH was adjusted to 4 using 0.1 M HCl to prevent copper precipitation occurring at pH above 6 (Carpio et al., 2014).

To examine the effect of surface functionalization and adsorbents dose, 2.5, 5.0, 10, 15, 20 mg of MC, O-MC, M-O-MC were added into conical tubes containing 10 mL of 50 mg/L copper solution. The tubes were shaken in a shaking incubator at 30 ℃ and 150 rpm for 12 hours.

The effect of contact time was investigated by adding 10 mg of M-O-MC into 10 mL of 50 mg/L copper solution (adsorbent dose = 1 g/L). The tubes were shaken in a shaker at 30 ℃ and 150 rpm and filtered after 0.17, 0.33, 0.5, 1, 3, 6, 12, 24 hours.

To observe the effect of initial copper concentration, copper stock solution was diluted to 25, 50, 100, 150, 200, 250 mg/L. 10 mg of M-O-MCs were added into 10 mL of each diluted copper solutions (adsorbent dose = 1 g/L) and were shaken in a shaker at 30 ℃ and 150 rpm for 12 hours.

To investigate the effect of temperature on copper removal, thermodynamic experiments were performed. 10 mg of M-O-MCs were added into 10 mL of copper

solution (initial concentration = 50 mg/L), and were shaken in a shaker at 15, 30, 45 ℃ and 150 rpm for 12 hours.

After reaction was completed, M-O-MCs were separated from the solution using 0.45 μm membrane filters, and initial and residual copper concentrations in solution were measured by inductively coupled plasma-atomic emission spectrometer (Optima- 4300 DV, PerkimElmer, USA).

All experiments were performed in duplicate.

3.4.2 Effect of solution composition

To investigate the effect of solution pH, copper solutions' pH were adjusted to 2, 3, 4, 5 using 0.1 M HCl and 0.1 M NaOH. M-O-MCs were added into the pH adjusted copper solutions (adsorbent dose : 1 g/L) and were shaken in a shaker at 30 ℃ and 150 rpm for 12 hours.

In order to examine the effect of ionic strength in copper adsorption onto M-O-MC, NaCl (Duksan), KCl (Duksan), NH_4Cl (Duksan), $CaCl_2$ (Daejung) were used as salts. Each salt was dissolved in 10 mL of 50 mg/L copper solutions in desired concentrations (0.01, 0.05, 0.1 M). 10 mg of M-O-MC was added into the above-mentioned solution (adsorbent dose : 1 g/L) and shaken in a shaker at 30 ℃ and 150 rpm for 12 hours.

To observe the competitive adsorption with other heavy metals, binary adsorption prepared by dissolving $CuCl_2 \cdot 2H_2O$ and $Ni(NO_3)2 \cdot 6H_2O$ (Duksan) in deionized water. Then, it was diluted in desired concentrations (25, 50, 100, 150, 200, 250 mg/L) and then shaken with M-O-MC (adsorbent dose : 1 g/L) at 30 ℃ and 150 rpm for 12 hours. Competition with zinc and cobalt was conducted similarly using $ZnSO_4 \cdot 7H_2O$ (Duksan) and $CoCl_2 \cdot 6H_2O$ (Duksan).

After reaction was completed, M-O-MC was separated from the solution using 0.45 μm membrane filters, and initial and residual copper (and nickel, zinc, cobalt in binary adsorption test) concentrations in solution were measured by inductively coupled plasma-atomic emission spectrometer.

3.4.3 Regeneration of M-O-MC and copper recovery

To determine the optimum solvent for adsorbed copper desorption, three different solvents were prepared; 0.1 M HCl, 0.1 M HNO_3. 50 mg of copper loaded M-O-MC was added into the 50 mL of each solvent and shaken in a shaker at 30 ℃ and 150 rpm for 1 hours.

In order to investigate the reusability of M-O-MC on copper removal, regeneration test was conducted. Copper adsorption-desorption cycle (initial copper concentration: 250 mg/L, adsorbent dose: 1 g/L) using M-O-MC was performed repeatedly 4 times.

Copper recovery was performed by precipitation process. Firstly, copper adsorption-desorption process was performed. Then copper desorbed solutions' pH were adjusted using 2 M NaOH solution. As precipitation proceeded by arising solution pH, precipitated iron oxide and copper oxide were filtered by 0.45 um membrane filtered, dried at 65 ℃, and analyzed by EDS to obtain element composition.

After reaction was completed, M-O-MC was separated from the solution using 0.45 μm membrane filters, and initial and residual copper and iron concentrations were measured by ICP-AES.

Figure 3-5. Shaking incubator

Figure 3-6. ICP-AES

3.5 Data analysis

The kinetic adsorption data can be analyzed by the following nonlinear forms of pseudo-first-order, pseudo-second-order, and Elovich models (Ho and Mckay, 1999; Mathialagan and Viraraghavan, 2003; Elovich and Larinov, 1962):

$$q_t = q_e[1 - \exp(-k_1 t)] \quad (1)$$

$$q_t = \frac{k_2 q_e^2 t}{1 + k_2 q_e t} \quad (2)$$

$$q_t = \frac{1}{\beta}\ln(\alpha\beta) + \frac{1}{\beta}\ln t \quad (3)$$

where q_t is the amount of contaminant adsorbed at time t, q_e is the amount of contaminant adsorbed at equilibrium, k_1 is the pseudo-first-order rate constant, k_2 is the pseudo-second-order rate constant, α is the initial adsorption rate constant and β is the Elovich adsorption constant.

The equilibrium adsorption data can be analyzed using the following nonlinear forms of Langmuir, Freundlich, Temkin, and Redlich-Peterson isotherm models (Foo and Hameed, 2010):

$$q_e = \frac{Q_m K_L C_e}{1 + K_L C_e} \quad (4)$$

$$q_e = K_F C_e^{\frac{1}{n}} \quad (5)$$

$$q_e = \frac{RT}{b_T} \ln(A_T C_e) \quad (6)$$

$$q_e = \frac{K_R C_e}{1 + a_R C_e^g} \quad (7)$$

where q_e is the amount of contaminant adsorbed at equilibrium, C_e is the equilibrium concentration of contaminant in the aqueous solution, Q_m is the maximum adsorption capacity, K_L is the Langmuir constant related to the affinity of the binding sites, K_F is the Freundlich constant related to the adsorption capacity, 1/n is the Freundlich constant related to the adsorption intensity, R is the gas constant (= 8.314 J/mol/K), T is absolute temperature, A_T is the Temkin isotherm equilibrium binding constant (L/g), b_T is the Temkin isotherm constant, K_R is the Redlich-Peterson constant related to the adsorption capacity, a_R is the Redlich-Peterson constant related to the affinity of the binding sites and g is the Redlich-Peterson constant related to the adsorption intensity.

The thermodynamic adsorption data can be analyzed by the following equations (Goswami and Purkait, 2011):

$$\Delta G^0 = \Delta H^0 - T\Delta S^0 \quad (8)$$

$$\Delta G^0 = -RT \, lnk_e \quad (9)$$

$$\ln(k_e) = \frac{\Delta S^0}{R} - \frac{\Delta H^0}{RT}; \; K_e = \frac{aq_e}{C_e} \quad (10)$$

where $\triangle G^0$ is the change in Gibb's free energy, $\triangle S^0$ is the change in entropy, $\triangle H^0$ is the change in enthalpy, R is the gas constant, K_e is the equilibrium constant (dimensionless), and a is the adsorbent dose (g/L). The values of $\triangle S^0$ and $\triangle H^0$ were determined by plotting ln(K_e) versus 1/T using Eq. (10) and the value of $\triangle G^0$ was calculated from Eq. (8).

All of the parameters of the models were estimated using MS Excel 2013 with the solver add-in function. The parameter values were determined by nonlinear regression. The determination coefficient (R^2), chi-square coefficient (χ^2), and sum of the absolute errors (SAE) were used to analyze the experimental data and confirm the fit to the model. The expressions of R^2, χ^2, SAE are the followings:

$$R^2 \frac{\sum_{i=1}^{m}(q_{e,calc} - \overline{q_{e,meas}})_i^2}{\sum_{i=1}^{m}(q_{e,calc} - \overline{q_{e,meas}})_i^2 + \sum_{i=1}^{m}(q_{e,calc} - q_{e,meas})_i^2} \quad (11)$$

$$\chi^2 = \sum_{i=1}^{m} \frac{(q_{e,meas} - q_{e,calc})^2}{q_{e,calc}} \quad (12)$$

$$\text{SAE} = \sum_{i=1}^{m} \left| q_{e,calc} - q_{e,meas} \right| \quad (13)$$

Where $q_{e,calc}$ is the calculated adsorption capacity from the model, $q_{e,meas}$ is the measured adsorption capacity from the experiment, and $\overline{q_{e,meas}}$ is the average of the measured adsorption capacity.

For the desorption study, desorption ratio was calculated according to the following equation:

$$\text{Desorption ratio (\%)} = \frac{Amount\ of\ metal\ ions\ desorbed}{Amount\ of\ metal\ ions\ adsorbed} \times 100 \qquad (14)$$

IV. Results and Discussion

4.1 Characteristics of mesoporous carbons

The digital image of M-O-MC presented in Figure 4-1 shows the black powdery particles. Figure 4-2 shows TEM images of MC, O-MC, and M-O-MC. As shown in Figure 4-2, nano-sized pores were observed regardless of surface functionalization. However, since acid-treatment and reaction with iron oxides proceeded, pores were partly blocked by oxygen and iron. From the EDS analysis data presented in Table 4-1, carbon is the primary element of MC. After treatment with nitric acid, oxygen content is increased over twice in O-MC (6.43 % to 15.43 %). Finally, attachment of iron oxide on the O-MC surface leads to increase oxygen and iron contents in M-O-MC.

After functionalization, decrease of surface area indicated in the N_2 adsorption-desorption isotherms results also can be understood in the same context. According to Table 4-2, MC had the BET specific surface area of 1488.10 m^2/g, total pore volume of 1.40 m^3/g, and mesopore area of 1251.00 m^2/g. As a result of surface oxidation, BET specific surface area, total pore volume, and mesopore area of O-MC decreased to 503.48 m^2/g, 0.37 m^3/g, and 273.31 m^2/g respectively due to pore blocking by oxygen. And finally, the bonds with iron blocked more pores, resulted in decrease of BET specific surface area, total pore volume, and mesopore area to 179.19 m^2/g, 0.18 m^3/g, 130.60 m^2/g. Surface area decrease also can be observed in preceding researches. Gu et al. (2007) observed the decrease in surface area of

mesoporous carbon after ion impregnation. Baikousi et al. (2012) also reported that specific surface area of mesoporous carbon decreased from 1650 m^2/g to 774 m^2/g after oxidation and reaction with iron oxide.

FT-IR spectra of mesoporous carbons is presented in Figure 4-3. They have several peaks in common at 3430, 2920, 1580, 1384 cm^{-1} associated with –OH stretching, C-H, C=O stretching in carboxylates, and O=C-O stretching in carboxylates respectively (Asouhidou et al., 2009). After treatment with nitric acid, the peaks at 1718 and 1228 cm^{-1} was observed indicating that C=O and –OH stretching of carboxylates were assigned (Moreno-Tovar et al., 2014, Asouhidou et al., 2009). The peak at 449 cm^{-1} was shown after reaction with iron oxide and can be attributed to the Fe-O bond of maghemite (Sharma & Jeevanandam, 2013).

From the XRD analysis result presented in Figure 4-4, mesoporous carbon has peaks at $2\Theta = 23°$ and $43°$ indicating amorphous carbon structure (Wang et al., 2009, Kim et al., 2003). After acid treatment, peaks were shifted because of surface oxidation. Finally, since O-MC reacted with iron oxide, the amorphous peaks diminished while peaks at (220), (311), (400) appeared which can be attributed to maghemite (Baikousi et al., 2012).

DLS analysis presented in Figure 4-5 and Table 4-2 indicates that M-O-MC particles had average size of 269.7 ± 31.4 nm. As shown in Figure 4-6, M-O-MC was attracted by magnet and shown its separability from aqueous solution.

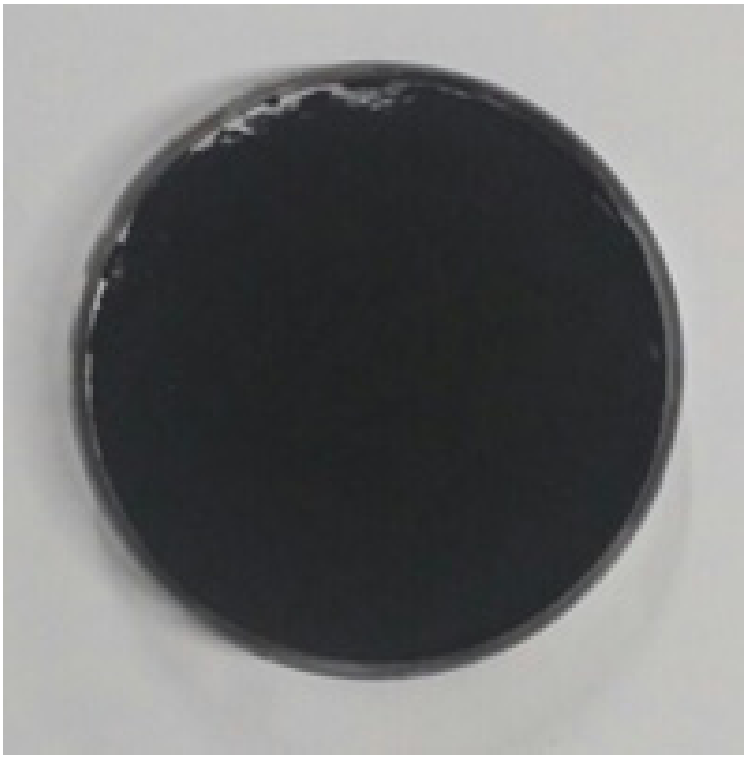

Figure 4-1. Digital image of M-O-MC

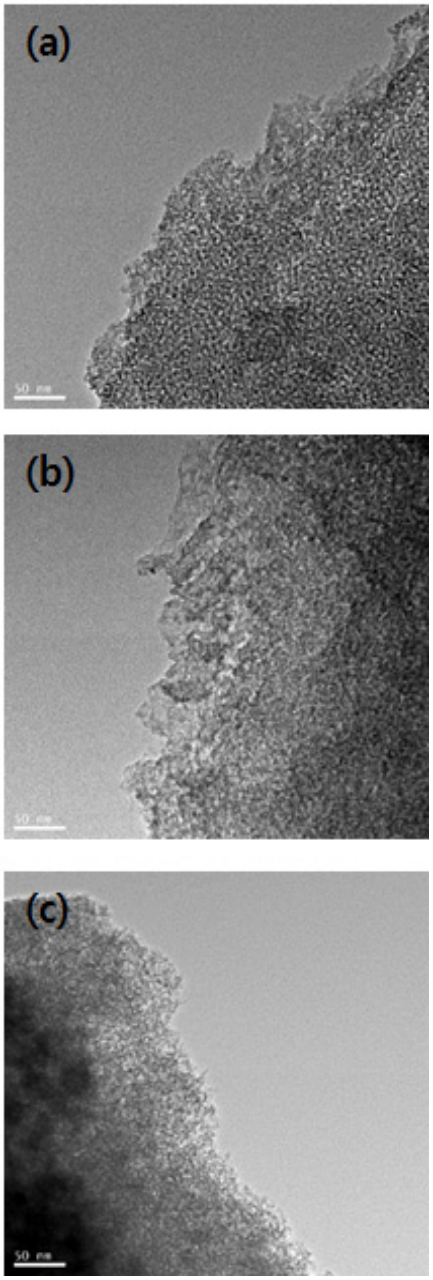

Figure 4-2. TEM images of (a) MC, (b) O-MC, and (c) M-O-MC

Table 4-1. EDS analysis results of mesoporous carbons

	Carbon (%)	Oxygen (%)	Iron (%)
MC	93.57	6.43	-
O-MC	84.87	15.13	-
M-O-MC	69.11	23.99	6.90

Table 4-2. N_2 gas adsorption-desorption analysis and DLS analysis results of mesoporous carbons

	Specific surface area (m^2/g)	Total pore volume (m^3/g)	Average pore diameter (nm)	Mesopore area (m^2/g)	Mesopore volume (m^3/g)	Size distribution (nm)
MC	1488.10	1.40	3.77	1251.00	1.20	184.7±47.5
O-MC	503.48	0.37	2.93	273.31	0.25	200.8±46.1
M-O-MC	179.19	0.18	4.01	130.60	0.15	231.8±62.7

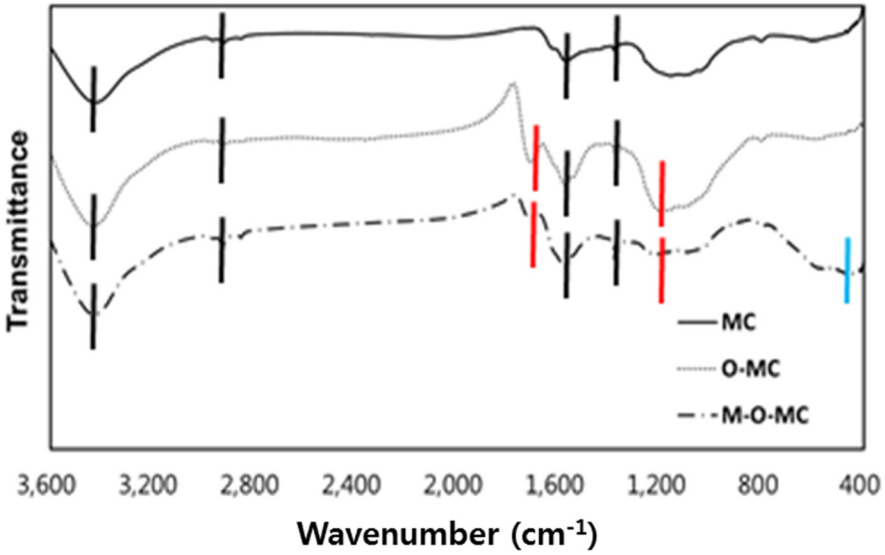

Figure 4-3. FT-IR spectra of mesoporous carbon

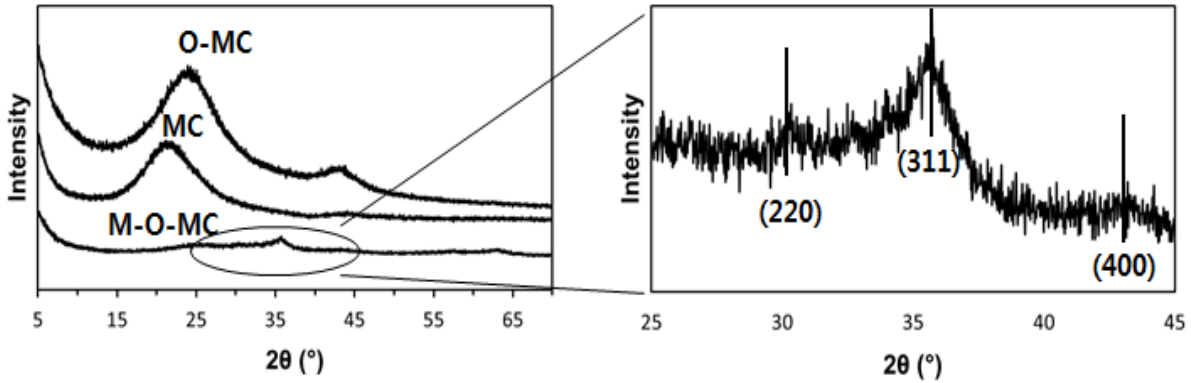

Figure 4-4. XRD Peaks of mesoporous carbons (left) and maghemite peaks of M-O-MC (right)

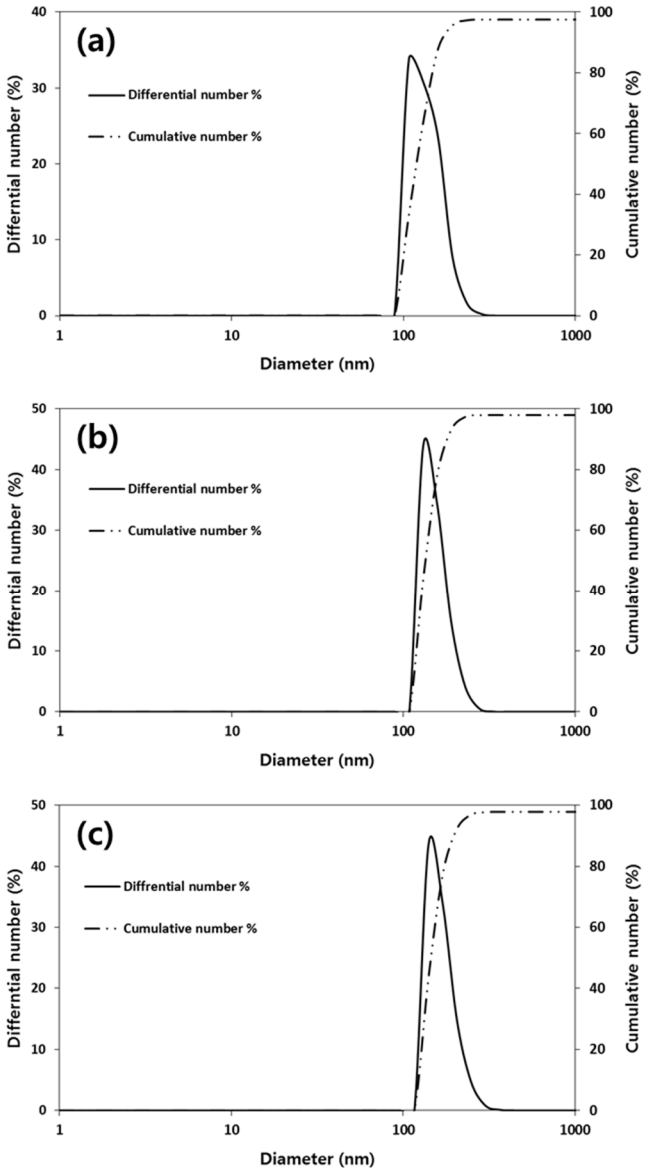

Figure 4-5. Size distribution of (a) MC, (b) O-MC, and (c) M-O-MC

Figure 4-6. Digital images of MC (left) and M-O-MC (right) under an external magnetic field

4.2 Copper ions removal and recovery in batch experiments results

4.2.1 Dose effect of adsorbents

The effect of MC, O-MC, and M-O-MC dose on the removal of copper ions is shown in Figure 4-7. At first, the removal percentage of copper ions gradually increased as the mass of adsorbents increased. The removal percentage of copper ions by MC, O-MC, M-O-MC respectively increased from 3.3±1.2 %, 24.9±0.35 %, 14.37±2.05 % to 15.5±0.1 %, 86.7±1.1 %, 96.8±1.5 % with increasing adsorbent dose from 0.25 to 2.00 g/L. It is considered that the more adsorption sites were provided to aqueous solution as the more adsorbents were added. Meanwhile, MC had the lowest copper ions adsorption capacity at all dose condition compared to O-MC and M-O-MC because of its hydrophobicity. After surface oxidation, O-MC and M-O-MC presented highly elevated copper ions adsorption capacity.

It is considered that surface carboxyl groups, structured during acid treatment process, contributed copper adsorption (Jaramillo et al., 2009). When M-O-MC dispersed in copper ions solution, H^+ of –COOH were exposed to the solution and $–COO^-$ were formed on the surface of M-O-MC. Then copper ions were adsorbed onto the surface M-O-MC combining with $–COO^-$. Schematic diagram of this process were presented in Figure 4-8. It is demonstrated by

Figure 4-9 indicating FT-IR spectra of M-O-MC and Cu-loaded M-O-MC respectively. Adsorption of copper ions onto M-O-MC resulted in diminishing and shifting of the peaks of carboxyl groups.

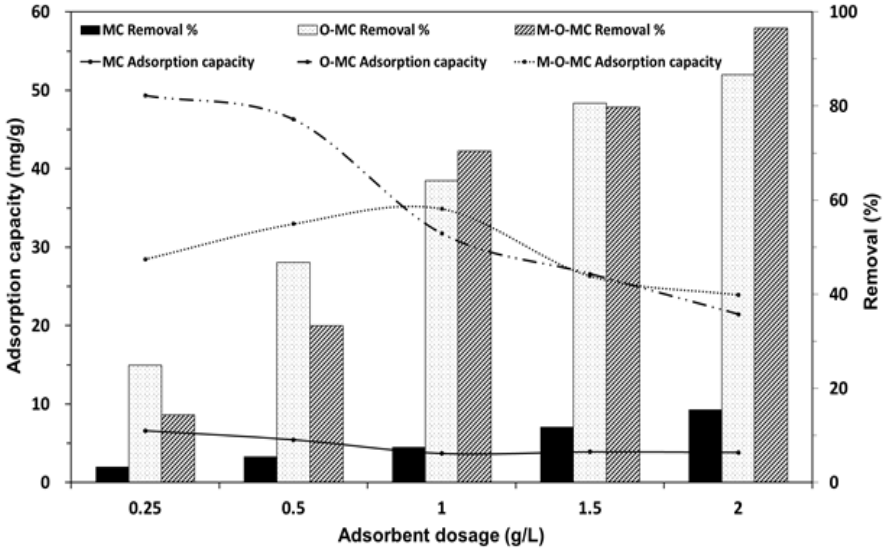

Figure 4-7. Effect of surface functionalization and dose of mesoporous carbons on the adsorption of copper ions

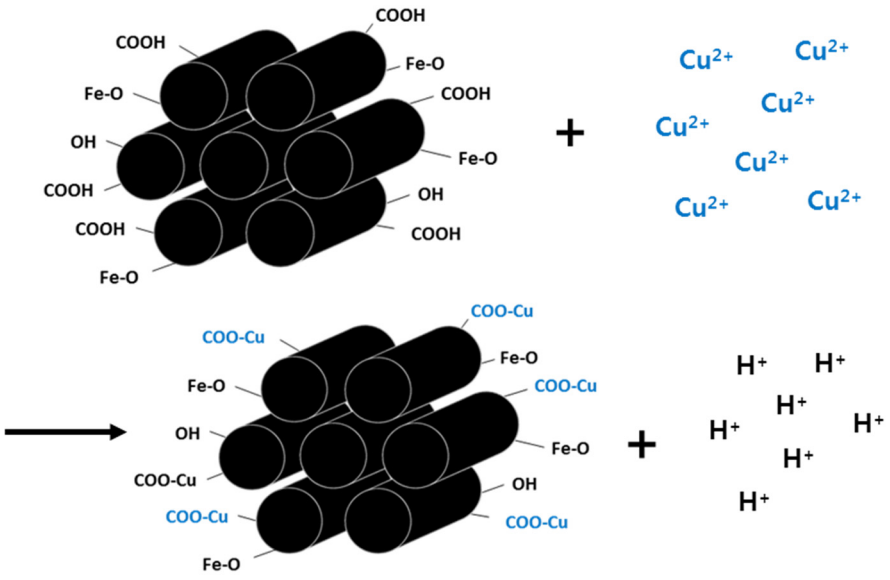

Figure 4-8. Schematic diagram of copper ions adsorption onto M-O-MC

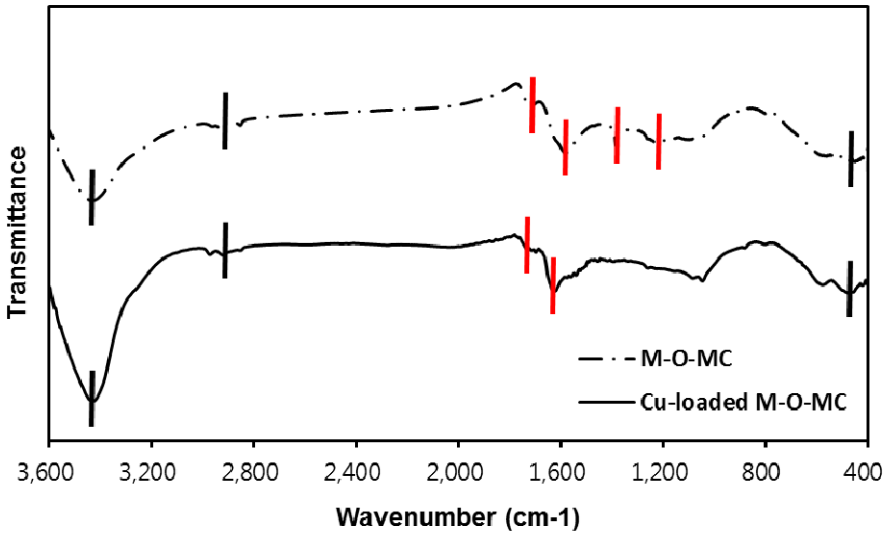

Figure 4-9. FT-IR spectra of M-O-MC and Cu-loaded M-O-MC

4.2.2 Effect of contact time

The effect of contact time on the adsorption of copper ions onto M-O-MC is presented in Figure 4-10. At the lowest initial concentration (50 mg/L), the adsorption capacity was 23.75±0.85 mg/g at 30 minutes of contact time. As reaction proceeded, the adsorption capacity gradually increased to 33.61±1.19 mg/g at 24 hours. At initial concentration of 100 mg/L, the adsorption capacity was 21.22±2.42 mg/g at 30 minutes and increased to 42.89±0.873 mg/g at 24 hours. At the highest initial concentration (250 mg/L), the adsorption capacity was 21.42±2.76 mg/g at 30 minutes, and increased to 45.43±2.02 mg/g at 24 hours. According to these results, other batch experiments were performed by mixing M-O-MC and copper solution for 12 hours to provide adequate reaction time.

The observed kinetic data were fitted by pseudo-first-order, pseudo-second-order, and Elovich model and shown in Figure 4-11. Model parameters are presented in Table 4-3. In the pseudo-first-order model fitting results, the values of q_e were 34.46, 44.18, 45.20 mg/g at the initial concentrations are 50, 100, 250 mg/L respectively. The values of k_1 were 2.34, 1.31, 1.39 (1/h) respectively. Pseudo-second-order model fitting results showed q_e values of 36.02, 43.77, 46.79 and k_2 values of 0.13, 0.09, 0.10 (1/h) respectively. In the Elovich model fitting results, the values of α were 1.22 E+7, 4.72 E+4, 1.75 E+4 and β were

0.51, 0.26, 0.22 respectively. From R^2, χ^2, and SAE values, kinetic data were well fitted by Pseudo-first-order model followed by Pseudo-second-order model, and Elovich model.

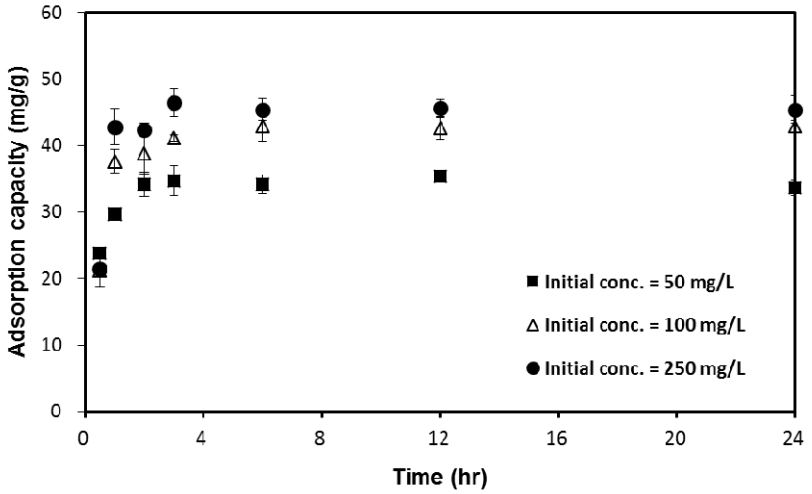

Figure 4-10. Effect of contact time on the adsorption of copper ions onto M-O-MC (adsorbent dose = 1 g/L, initial pH = 4)

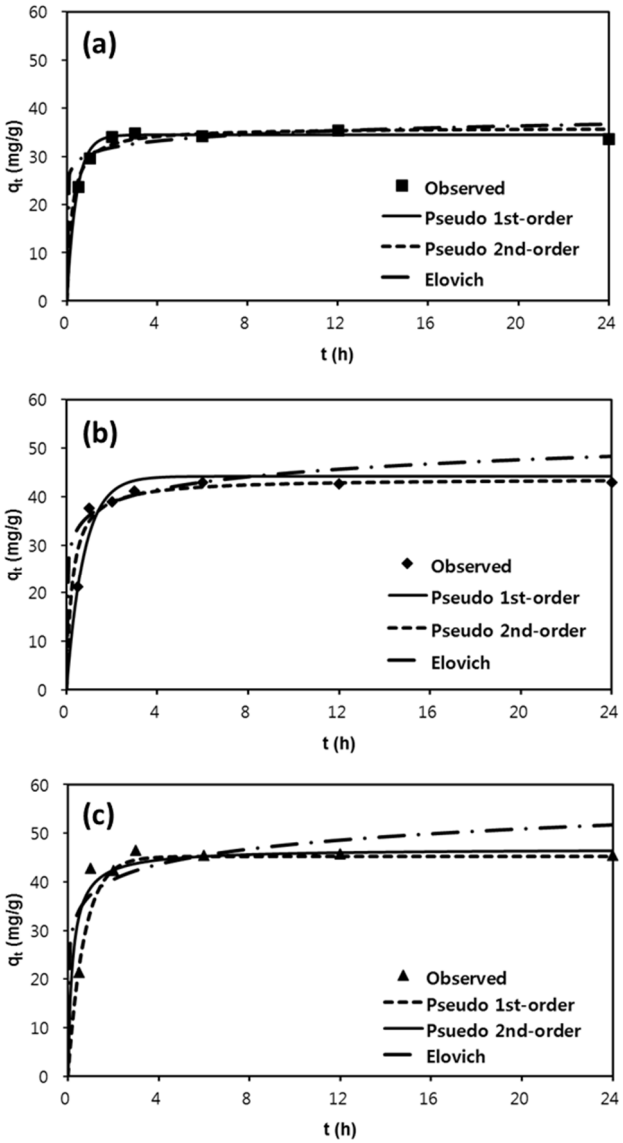

Figure 4-11. Kinetic data and model fits for copper ions removal by M-O-MC: (a) model fit at initial conc. of 50 mg/L, (b) model fit at initial conc. of 100 mg/L, and (c) model fit at initial conc. of 250 mg/L

Table 4-3. Kinetic model parameters obtained from model fitting (Pseudo-first order, Pseudo-second order and Elovich model)

Conc. (mg/L)	Pseudo-first-order model					Pseudo-second-order model					Elovich model				
	q_e (mg/g)	k_1 (1/h)	R^2	χ^2	SAE	q_e (mg/g)	k_2 (g/mg/h)	R^2	χ^2	SAE	a (mg/g/h)	b (g/mg)	R^2	χ^2	SAE
50	34.46	2.34	0.965	0.120	3.846	36.02	0.13	0.919	1.326	6.874	1.22E+07	0.51	0.573	1.593	13.907
100	44.18	1.31	0.913	1.245	13.755	43.77	0.09	0.889	2.386	12.975	4.72E+04	0.26	0.615	5.334	23.146
250	45.20	1.39	0.859	2.455	13.042	46.79	0.10	0.803	4.741	19.918	1.75E+04	0.22	0.484	7.018	33.557

4.2.3 Effect of initial copper concentration

The effect of initial copper concentration on the adsorption of copper ions onto M-O-MC is shown in Figure 4-12. At the lowest concentration of 25 mg/L, the adsorption capacity values were 31.74±0.49, 24.44, 12.22 mg/g and percent removals were 64.93±2.00, 100, 100 % at adsorbent dose of 0.5, 1, 2 g/L respectively. As copper concentration increased to 250 mg/L, the adsorption capacity values increased to 49.23±6.00, 46.38±1.89, 43.80±2.01 mg/g and percent removals decreased to 9.70±2.36, 18.28±0.74, 34.52±0.81 % respectively. At low concentration, copper ions were not sufficient to fill up the adsorption sites on the M-O-MC. At higher concentration, adsorption of copper ions onto M-O-MC was performed enough and resulted in increase of adsorption capacity.

The equilibrium data were fitted by Langmuir isotherm, Freundlich isotherm, Temkin isotherm, and Redlich-Peterson isotherm model and shown in Figure 4-13. Model parameters are presented in Table 4-4 and Table 4-5. In the Langmuir isotherm model, the maximum adsorption capacity values (Q_m) were 51.424, 48.354, 46.427 mg/g at adsorbent dose of 0.5, 1, 2 g/L respectively. In the Freundlich isotherm model, the distribution coefficients (K_F) were 23.020, 26.952, 36.745 L/g at adsorbent dose of 0.5, 1, 2 g/L respectively. From the Temkin isotherm model, (A_T) were 64.871, 292.505, 884.303 L/g at adsorbent dose of 0.5, 1, 2 g/L respectively. And in the

Redlich-Peterson isotherm model, parameter values of K_R/a_R were 506, 46.821, 42.518 mg/g g at adsorbent dose of 0.5, 1, 2 g/L respectively. The overall values of R^2, χ^2, and SAE suggested that the Freundlich isotherm model was appropriate for describing the equilibrium data of copper adsorption onto M-O-MC.

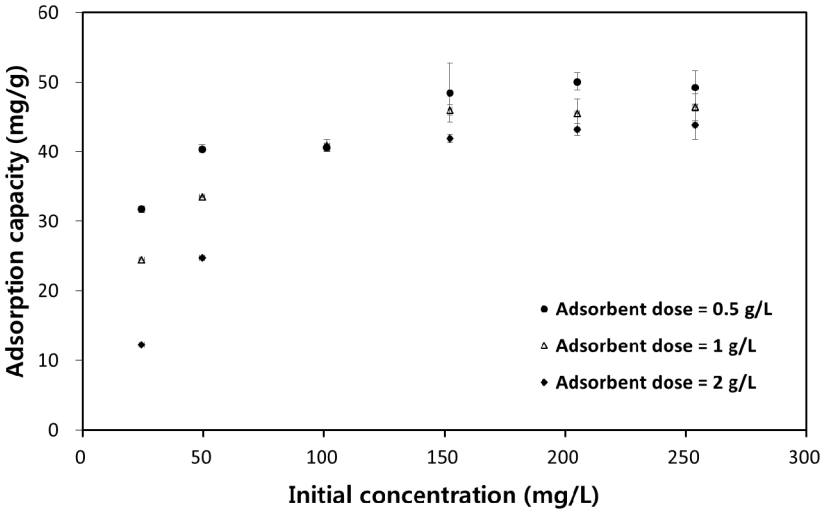

Figure 4-12. Effect of initial copper concentration on the adsorption of copper ions onto M-O-MC (contact time = 12 h, initial pH = 4)

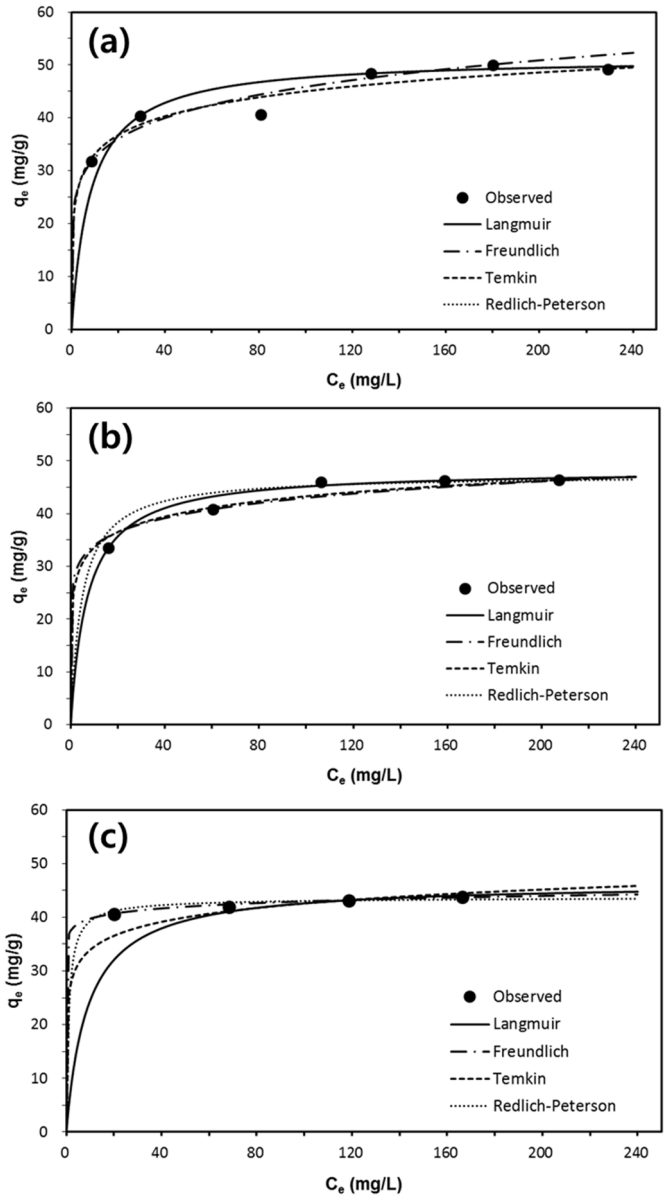

Figure 4-13. Equilibrium data and model fits for copper ions removal by M-O-MC: (a) adsorbent dose: 0.5 g/L, (b) adsorbent dose: 1 g/L, (c) adsorbent dose: 2 g/L

Table 4-4. Equilibrium model parameters (Langmuir and Freundlich isotherm model) obtained from model fitting

M-O-MC dose (g/L)	Langmuir isotherm model					Freundlich isotherm model				
	Q_m (mg/g)	K_L (L/mg)	R^2	χ^2	SAE	K_F (L/g)	1/n	R^2	χ^2	SAE
0.5	51.424	0.125	0.854	1.821	12.580	23.020	0.150	0.893	0.601	9.520
1	48.354	0.141	0.957	0.143	3.424	26.952	0.102	0.945	0.335	6.067
2	46.427	0.112	0.868	2.330	9.705	36.745	0.034	0.964	0.006	0.617

Table 4-5. Equilibrium model parameters (Temkin and Redlich-Peterson isotherm model) obtained from model fitting

M-O-MC dose (g/L)	Temkin isotherm model					Redlich-Peterson isotherm model				
	A_T (L/g)	b_T (J/mol)	R^2	χ^2	SAE	K_R/a_R (mg/g)	g	R^2	χ^2	SAE
0.5	64.871	491.849	0.917	0.518	9.825	51.424	1.000	0.854	1.821	12.580
1	292.505	598.484	0.956	0.285	5.842	45.217	0.990	0.961	0.113	3.385
2	884.303	675.048	0.960	0.492	5.547	42.518	0.995	0.904	0.032	1.948

4.2.4 Effect of temperature

The effect of temperature on the adsorption of copper ions onto M-O-MC was evaluated by thermodynamic analysis. The results are presented in Figure. 4-14 and Table 4-6. The positive values of ΔH° demonstrate that copper ions adsorption is endothermic reaction. Also, ΔS° values is also positive indicating that the randomness between solid and solution increases during the adsorption process. And the negative values of ΔG° means that the adsorption process is spontaneous. However, Anbia and Haqshenas (2015) reported the different result. According to their research, copper ions adsorption onto mesoporous carbon nitride functionalized with melamine-based dendrimer amine (MDA-MCN-1) was hindered by the increasing temperature from 50 to 20 ℃. So the adsorption of copper ions onto MDA-MCN-1 was exothermic process. Meanwhile, Li and Ren (2015) reported that the adsorption of copper ions onto nitrogen-functionalized mesoporous carbon reached its peak at 40 ℃, but decreased at higher temperature. They explained this result that high temperature resulted in the escape of copper ions from the surface of adsorbent.

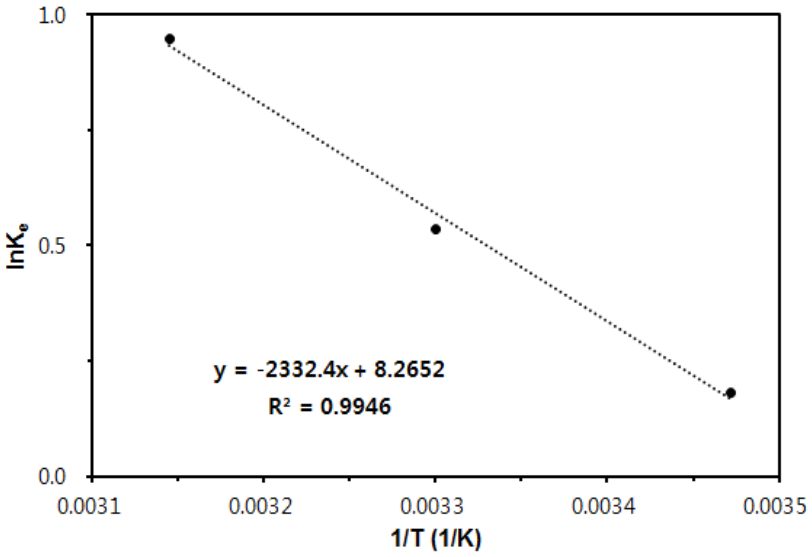

Figure 4-14. Thermodynamic analysis for copper ions adsorption onto M-O-MC

Table 4-6. Thermodynamic parameters for copper ions adsorption onto M-O-MC

Temperature (℃)	ΔH°	ΔS°	ΔG°
15			-0.40
30	19.41	68.75	-1.43
45			-2.46

4.2.5 Comparison with preceding studies

There were some preceding researches studying copper adsorption onto functionalized mesoporous carbon. In Table 4-7, each research's copper adsorption capacity values at optimum conditions were summarized. From the table, M-O-MC prepared in the present study shows relatively higher copper adsorption capacity than literatures except for reports of Li & Ren (2015) and Anbia & Haqshenas (2015). Li & Ren (2015) and Anbia & Haqshenas (2015) observed relatively higher adsorption capacity than this study's result. It might be resulted from the different surface functionalization of mesoporous carbon and different experimental conditions such as high initial pH or high temperature which are more favorable conditions for copper adsorption than this study.

Table 4-7. Comparison of the copper adsorption by functionalized mesoporous carbon with preceding studies

References	Functionalization	Dosage (g/L)	Initial concentration (mg/L)	Equilibrium reached time (min)	Initial pH	Temperature (℃)	Adsorption capacity (mg/g)
Baikousi et al. (2013)	Carbonyl	-	24	40	< 5.0	-	24
Chen et al. (2014)	Magnetically separable N-doped	1	50	360	4.0	25	24
Anbia & Haqshenas (2015)	Dendrimer amine	0.5	100	20	8.0	20	200
Barczak et al. (2015)	Amino	5	80	15	5.0	25	43
Guo et al. (2015)	8-HQ-Ni	2	5	10	5.0	25	3
Li & Ren (2015)	Nitrogen	0.4	50	360	5.6	40	117
This study	Magnetic-oxidized	1	250	180	4.0	30	48

4.2.6 Effect of solution pH, ionic strength, and other heavy metals

The effect of solution pH on the adsorption of copper ions onto M-O-MC was investigated and shown in Figure 4-15. The adsorption capacity of copper ions at pH 4, 5 were 40.87±1.49, 50.46±0.25 mg/g respectively. When initial solution pH decreased from 3 to 2, the adsorption capacity also decreased from 14.93±0.46 to 1.12±0.10 mg/g respectively. At strong acidic condition, copper ions compete with protons for adsorption sites on the M-O-MC. It resulted in decrease of adsorption capacity at acidic condition. Meanwhile, about 97% of copper ions were removed at initial pH 5. At this point, final pH rose up to 6.12, so high removal percentage of copper ions were resulted from not only adsorption onto M-O-MC, but also precipitation as a form of $Cu(OH)_2$.

The effect of ionic strength on the adsorption of copper ions onto M-O-MC is shown in Figure 4-16. The results indicate that the presence of electrolytes such as $CaCl_2$, NaCl, KCl, NH_4Cl resulted in reduction of copper adsorption capacity. Also, the higher concentration of electrolytes was, the lower adsorption capacity resulted. It is considered that copper ions competed with electrolytes cations for adsorption sites on the M-O-MC (Jiang et al., 2010). Meanwhile, the influence of cation to copper adsorption is in order of Ca^{2+} > K^+ > Na^+ > NH_4^+. Especially, Ca^{2+}, the divalent cation, had more negative effect on the adsorption of copper ions than monovalent cations. This result suggested

that divalent cation has stronger preference with the adsorbent than monovalent cation (Adebowale et al., 2006).

Binary adsorption test was performed to observe the effect of other heavy metals on copper ions adsorption onto M-O-MC. From the Figure 4-17, M-O-MC shows selective adsorption property for copper ions better than nickel, zinc, and cobalt ions. As initial concentration of metal ions increased, the gap of adsorption capacity between copper and other heavy metals became more obvious. It suggests that M-O-MC has relatively higher affinity adsorption site for copper ions than nickel, zinc, and cobalt ions. The higher adsorption capacity of copper ions could be resulted from its physico-chemical properties such as electronegativity and ionic radii. According to Krishnan et al.(2002), metal ions' affinity to the adsorbent increase when their ionic radius become bigger. Meanwhile, the increase of metals' electronegativity also results in higher adsorption capacity (Zhang, 2011). As shown in Table 4-8, copper has higher electronegativity and larger ionic radius than nickel, zinc, and cobalt. Therefore, results of the binary adsorption test in this study might be reasonable. As a result, M-O-MC can be used for separation of copper ions from the solution containing nickel, zinc, and cobalt ions.

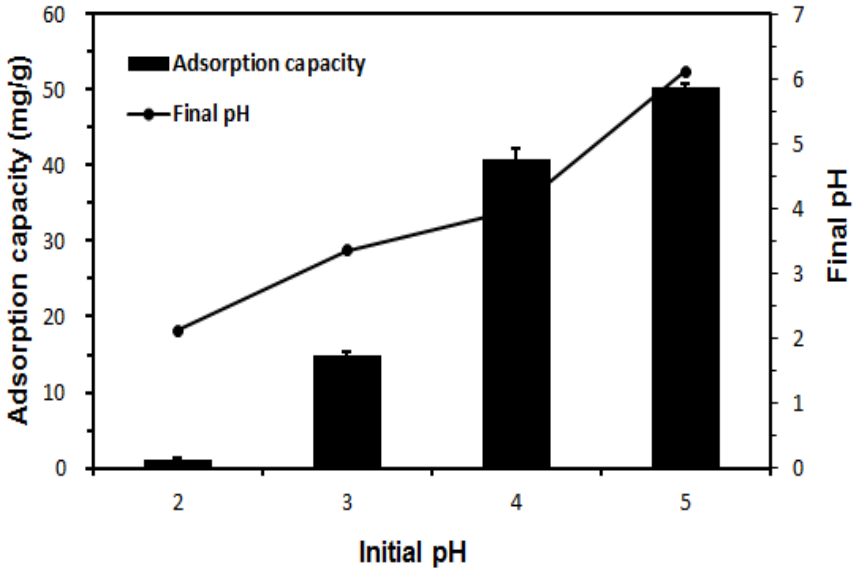

Figure 4-15. Effect of initial solution pH on the adsorption of copper ions onto M-O-MC (adsorbent dose = 1 g/L, initial conc. = 50 mg/L)

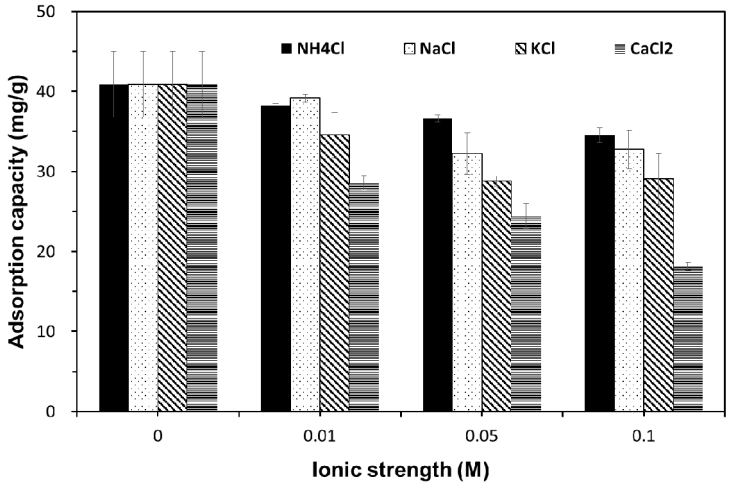

Figure 4-16**.** Effect of ionic strength on the adsorption of copper ions onto M-O-MC (adsorbent dose = 1 g/L, initial pH = 4)

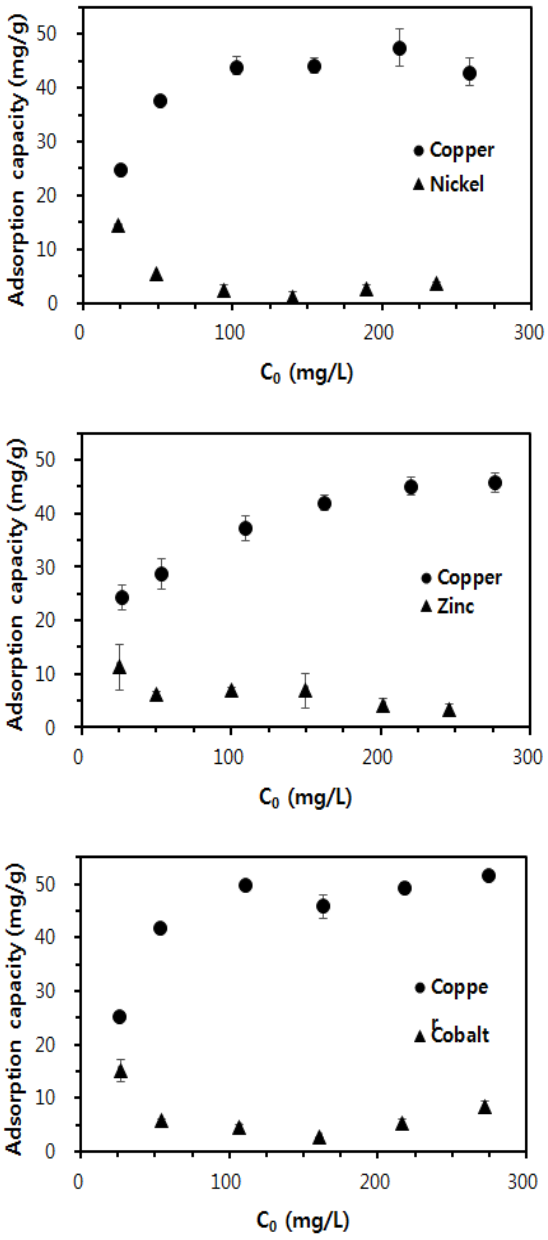

Figure 4-17. Effect of other heavy metals on the adsorption of copper ions onto M-O-MC (adsorbent dose = 1 g/L, initial pH = 4)

Table 4-8. Electronegativity and ionic radius of Cu(II), Ni(II), Zn(II) ad Co(II)

	Electronegativity [a]	Ionic radius (Å) [b]
Cu (II)	2.0	0.96
Ni (II)	1.8	0.78
Zn (II)	1.6	0.83
Co (II)	1.8	0.82

[a] obtained from Dastgheib et al.(2002)

[b] obtained from Shackelford and Alexander (2000)

4.2.7 Regeneration of M-O-MC and copper recovery test

Copper desorption test was conducted firstly to determine the optimum solvent for copper desorption. As shown in Figure 4.18, strong acidic solutions (0.1 M HCl, 0.1 M HNO_3) indicate high desorption rate. HCl, HNO_3 desorbed 100, 94.91% of copper ions adsorbed onto M-O-MC respectively. Therefore, HCl was selected for desorption solvent and used at following experiments.

Regeneration of M-O-MC in copper adsorption was performed using 0.1 M HCl as desorption solvent. As shown in Figure 4-19, it is observed that the adsorption capacity of copper ions reduced by half after first cycle. The adsorption capacity was 43.29±0.67 mg/g at 1^{st} cycle and decreased to 18.43±0.48 mg/g at 2^{nd} cycle. Then, the adsorption capacity slightly changed to 18.57±0.38 mg/g and 15.98±0.40 mg/g at 3^{rd} and 4^{th} cycle respectively.

It is considered that this tendency can be associated with solution pH. Prior to reuse, copper loaded M-O-MC was treated with 0.1 M HCl to desorb copper ions. Although rinsing M-O-MC with deionized water was performed before reuse, HCl treated M-O-MC released more H^+ than the initially prepared M-O-MC. As a result, solution pH slightly dropped after reuse of M-O-MC, and resulted in reduction of adsorption capacity of copper.

Copper recovery test was performed by precipitation. In the process of desorption using acidic solution, iron on the M-O-MC surface as well as copper adsorbed onto M-O-MC leached to solution. Therefore, it is necessary to

separate both metals to recover pure copper. In order to solve this problem, metals' unique characteristic was adopted. Metal ions in aqueous solution form different metal speciations according to pH variation. Based on this principle, leached iron ions and desorbed copper ions from M-O-MC were sequentially separated from the solution. As shown in Figure 4-20, iron ions were precipitated firstly from pH 5, and then copper ions were precipitated later from pH 6. From the table 4-9, precipitates were identified as iron oxide and copper oxide respectively. Figure 4-21 shows the digital image of precipitated copper.

As shown in Figure 4-22, magnetic characteristic of M-O-MC was maintained after repeatedly use for 4 times, although there were iron leaching during desorption process.

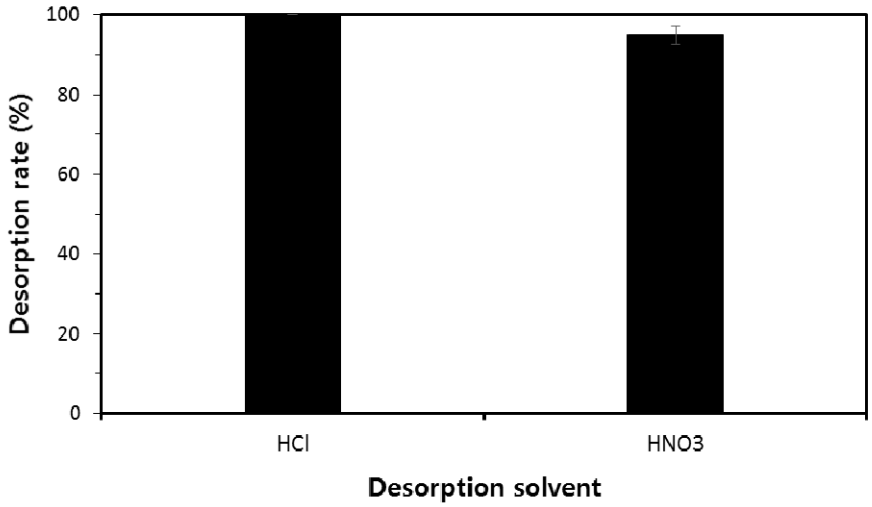

Figure 4-18. Desorption rate of copper ions loaded onto M-O-MC by solvent type

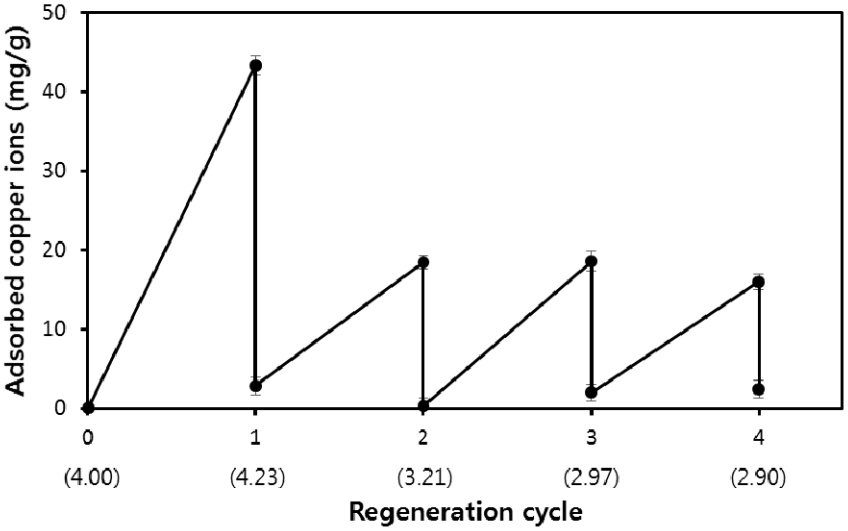

Figure 4-19. Repeated use of M-O-MC in copper ions adsorption
(the numbers in the parenthesis of X-axis: final pH)

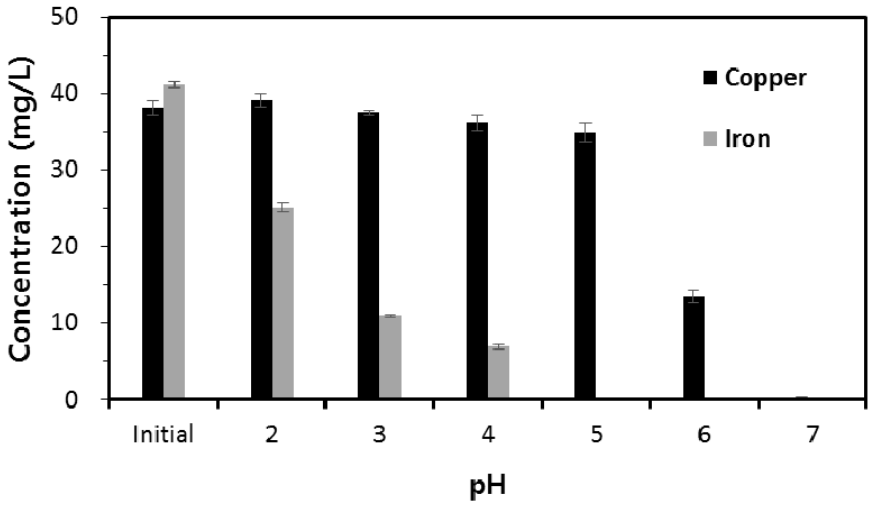

Figure 4-20. Sequential separation of iron and copper ions by pH variations

Table 4-9. EDS analyses results of iron and copper precipitations

	Iron (%)	Copper (%)	Oxygen (%)	Chloride (%)
Iron precipitation	31.57	3.52	59.41	5.49
Copper precipitation	-	34.30	57.93	7.77

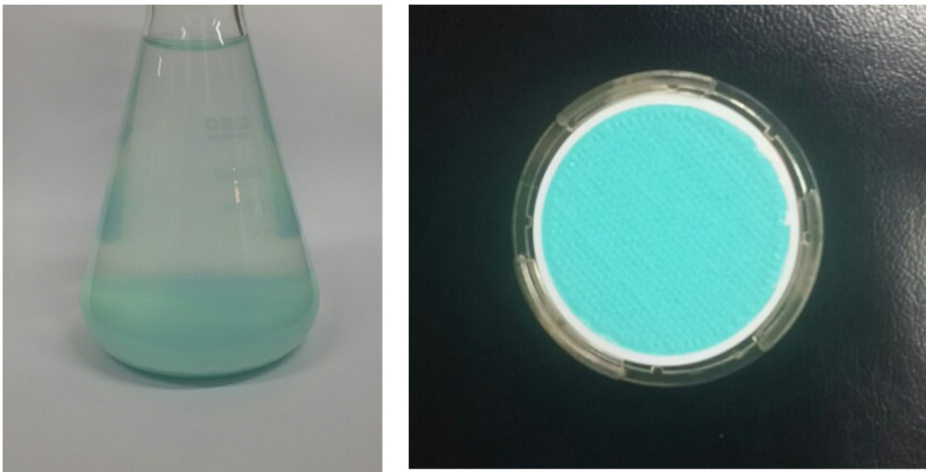

Figure 4-21. Digital image of precipitated and filtered copper

Figure 4-22. Digital image of repeatedly used M-O-MC under an external magnetic field

V. Conclusions

In this study, magnetic-oxidized-mesoporous-carbon was synthesized and applied for copper removal and recovery. The adsorption capacity of copper ions onto mesoporous carbon increased as surface functionalization proceeded. From the kinetic test, adsorption of copper ions onto M-O-MC increased as contact time went on and the data were well fitted by Pseudo-first-order model. According to the equilibrium test, data were well described by Freundlich isotherm model and the maximum adsorption capacity was calculated to 48.354 mg/g from Langmuir isotherm model at M-O-MC dose of 1 g/L. Thermodynamic test indicated that reaction between copper ions and M-O-MC is endothermic and spontaneous. When initial solution pH decreased to strong acidic condition, adsorption capacity also decreased because of competition with protons. Ionic strength also had an effect on the adsorption of copper ions onto M-O-MC. As ionic strength increased, adsorption capacity decreased due to competition with salt cations. Meanwhile, copper ions had stronger affinity with M-O-MC than nickel, zinc, and cobalt ions. Desorption test and regeneration study showed the reusability of M-O-MC in copper ions removal. Leached iron ions and desorbed copper ions from M-O-MC were sequentially separated from aqueous solution by precipitation method raising solution pH. This study demonstrated that M-O-

MC can be applied as adsorbents for removing and recovering copper ions from aqueous solution.

VI. References

Adebowale KO, Unuabonah IE, Olu-Owolabi BI. 2006. The effect of some operating variables on the adsorption of lead and cadmium ions on kaolinite clay. *Journal of Hazardous Materials* **B134**: 130-139.

Ahmad AL, Ooi BS. 2010. A study on acid reclamation and copper ecovery using low pressure nanofiltration membrane. *Chemical Engineering Journal* **156**: 257-263.

Anbia M, Amirmahmoodi S. 2011. Removal of Hg (II) and Mn (II) from aqueous solution using nanoporous carbon impregnated with surfactants, *Arabian Journal of Chemistry*.

Anbia M, Dehghan R. 2014. Functionalized CMK-3 mesoporous carbon with 2-amino-5-mercapto-1,3,4-thiadiazole for Hg (II) removal from aqueous media. *Journal of Environmental Sciences* **26**: 1541-1548.

Anbia M, Haqshenas M. 2015. Adsorption studies of Pb(II) and Cu(II) ions on mesoporous carbon nitride functionalized with melamine-based dendrimer amine. *International Journal of Environmental Science and Technology* **12**: 2649-2664.

Asouhidou DD, Triantafyllidis KS, Lazaridis NK, Matis KA, Kim SS, Pinnavaia TJ. 2009. Sorption of reactive dyes from aqueous solutions by ordered hexagonal and disordered mesoporous carbons. *Microporous and Mesoporous Materials* **117**: 257-267.

Baikousi M, Bourlinos AB, Douvalis A, Bakas T, Anagnostopoulos DF, Tuček J, Šafářová K, Zboril R, Karakassides MA. 2012. Synthesis and Characterization of -Fe2O3/Carbon Hybrids and Their Application in Removal of Hexavalent Chromium Ions from Aqueous Solutions. *Langmuir* **28**: 3918-3930.

Baikousi M, Daikopoulos C, Georgiou Y, Bourlinos A, Zbořil R, Deligiannakis Y, Karakassides MA. 2013. Novel Ordered Mesoporous Carbon with Innate Functionalities and Superior Heavy Metal Uptake. *The Journal of Physical Chemistry* **117**: 16961-16971.

Baikousi M, Georgiou Y, Daikopoulos C, Bourlinos AB, Filip J, Zboril R, Deligiannakis Y, Karakassides MA. 2015. Synthesis and characterization of

robust zero valent iron/mesoporous carbon composites and their applications in arsenic removal. *Carbon* **93**: 636-647.

Baniamerian MJ, Moradi SE, Noori A, Salahi H. 2009. The effect of surface modification on heavy metal ion removal from water by carbon nanoporous adsorbent. *Applied Surface Science* **256**: 1347-1354.

Barczak M, Michalak-Zwierz K, Gdula K, Tyszczuk-Rotko K, Dobrowolski R, Dąbrowski A. 2015. Ordered mesoporous carbons as effective sorbents for removal of heavy metal ions. *Microporous and Mesoporous Materials* **211**: 162-173.

Boujelben N, Bouzid J, Elouear Z. 2009. Adsorption of nickel and copper onto natural iron oxide-coated sand from aqueous solutions: study in single and binary systems. *Journal of Hazardous Materials* **163**: 376-382.

Chang H, Joo SH, Pak C. 2007. Synthesis and characterization of mesoporous carbon for fuel cell applications. *Journal of Materials Chemistry* **17**: 3078-3088.

Chen A, Yu Y, Zhang Y, Xing T, Wang Y. 2014. Solid-solid grinding/templating route to magnetically separable nitrogen-doped mesoporous carbon for removal Cu^{2+} ions. *Journal of Hazard Materials* **279**: 280-288.

Chen H, Yan T, Jiang F. 2014. Adsorption of Cr(VI) from aqueous solution on mesoporous carbon nitride. *Journal of the Taiwan Institute of Chemical Engineers* **45**: 1842-1849.

Chen T, Wang T, Wang DJ, Xue HR, Zhao JQ, Ding XC, Wu SC, He JP. 2011. Synthesis of ordered large-pore mesoporous carbon for Cr(VI) adsorption. *Materials Research Bulletin* **46**: 1424-1430.

Dai Y, Hu Y, Jiang B, Zou J, Tian G, Fu H. 2015. Carbothermal synthesis of ordered mesoporous carbon-supported nano zero-valent iron with enhanced stability and activity for hexavalent chromium reduction. *Journal of Hazardous Materials*.

Dastgheib SA, Rockstraw DA. 2002. A model for the adsorption of single metal ion solutes in aqueous solution onto activated carbon produced from pecan shells. *Carbon* **40**: 1843-1851.

Carpio IEM, Mangadlao JD, Nguyen HN, Advincula RC, Rodrigues DF. 2014. Graphene oxide functionalized with ethylenediamine triacetic acid for heavy metal adsorption and anti-microbial applications. *Carbon* **77**: 289-301.

Elovich SY, Larionov OG. 1962. Theory of adsorption from solutions of non electrolytes on solid (I) equation adsorption from solutions and the analysis of its simplest form, (II) verification of the equation of adsorption isotherm from solutions. *Izvestiya Akademii Nauk SSSR, Otdelenie Khimicheskikh Nauk* **2**: 209-216.

Foo KY, Hameed BH. 2010. Insights into the modeling of adsorption isotherm systems. *Chemical Engineering Journal* **156**: 2-10.

Goswami A, Purkait MK. 2011. Kinetic and equilibrium study for the fluoride adsorption using pyrophyllite. *Separation Science and Technology* **46**: 1797-1807

Gu Z, Deng B, Yang J. 2007. Synthesis and evaluation of iron-containing ordered mesoporous carbon (FeOMC) for arsenic adsorption. *Microporous and Mesoporous Materials* **102**: 265-273.

Gu Z, Deng B. 2007. Arsenic sorption and redox transformation on iron-impregnated ordered mesoporous carbon. *Applied Organometallic Chemistry* **21**: 750-757.

Guo W, Meng X, Liu Y, Ni L, Hu Z, Chen R, Meng M, Wang Y, Han J, Luo M. 2015. Synthesis and application of 8-hydroxyquinoline modified magnetic mesoporous carbon for adsorption of multivatiate metal ions from aqueous solutions. *Journal of Industrial and Engineering Chemistry* **21**: 340-349.

Ho YS, McKay G. 1999. Pseudo-second order model for sorption processes. *Process Biochemistry* **34**: 451-465.

Hu XJ, Liu YG, Wang H, Chen AW, Zeng GM, Liu SM, Guo YM, Hu X, Li TT, Wang YQ, Zhou L, Liu SH. 2013. Removal of Cu(II) ions from aqueous solution using sulfonated magnetic graphene oxide composite. *Separation and Purification Technology* **108**: 189-195.

Huang CC, He JC. 2013. Electrosorptive removal of copper ions from wastewater by using ordered mesoporous carbon electrodes. *Chemical Engineering Journal* **221**: 469-475.

Jaramillo J, Gómez-Serranob V, Álvarez PM. 2009. Enhanced adsorption of metal ions onto functionalized granular activated carbons prepared from cherry stones. *Journal of Hazardous Materials* **161**: 670-676.

Jiang M, Jin X, Lu X, Chen Z. 2010. Adsorption of Pb(II), Cd(II), Ni(II) and Cu(II) onto natural kaolinite clay. *Desalination* **252**: 33-39.

Joo JB, Kim P, Kim W, Kim J, Yi J. 2006. Preparation of mesoporous carbon templated by silica particles for use as a catalyst support in polymer electrolyte membrane fuel cells. *Catalysis Today* **111**: 171-175.

Keane MA. 1998. The removal of copper and nickel from aqueous solution using Y zeolite ion exchangers. *Colloids and Surfaces A: Physicochemical and Engineering Aspects* **138**: 11-20.

Kim TW, Park IS, Ryoo R. 2003. A synthetic route to ordered mesoporous carbon materials with graphitic pore walls. *Angewandte Chemie* **115**: 4511-4515.

Krishnan KA, Anirudhan TS. 2002. Uptake of heavy metals in batch systems by sulfurized steam activated carbon prepared from sugarcane bagasse pith. *Industrial & Engineering Chemistry Research* **41**: 5085-5093.

Li Z, Ren S. 2015. Preparation of nitrogen-functionalized mesoporous carbon and its application for removal of copper ions. *Journal of Materials Science* **50**: 4600-4609.

Lu L, Zhao H, Yan L, Wang G, Mao Y, Wang X, Liu K, Liu X, Zhao Q, Jiang T. 2015. Removal characteristics of Cd(II) ions from aqueous solution on ordered mesoporous carbon. *Korean Journal of Chemical Engineering* **32**: 2161-2167.

Mathialagan T, Viraraghavan T. 2003. Adsorption of cadmium from aqueous solutions by vermiculite. *Separation Science and Technology* **38**: 57

Mi X, Huang G, Xie W, Wang W, Liu Y, Gao J. 2012. Preparation of graphene oxide aerogel and its adsorption for Cu^{2+} ions. *Carbon* **50**: 4856-4864.

Mineral commodity summaries. 2010. U.S. Geological Survey.

Mirbagheri SA, Hosseini SN. 2004. Pilot plant investigation on petrochemical wastewater treatment for the removal of copper and chromium with the objective of reuse. *Desalination* **171**: 85-93.

Moreno-Tovar R, Terrés E, Rangel-Mendez JR. 2014. Oxidation and EDX elemental mapping characterization of an ordered mesoporous carbon: Pb(II) and Cd(II) removal. *Applied Surface Science* **303**: 373-380.

Ochoa-Herrera V, Leon G, Banihani Q, Field JA, Sierra-Alvarez R. 2011. Toxicity of copper(II) ions to microorganisms in biological wastewater treatment systems. *Science of the Total Environment* **412-413**: 380-385.

Özer A, Özer D, Özer A. 2003. The adsorption of copper(II) ions on to dehydrated wheat bran (DWB): determination of the equilibrium and thermodynamic parameters. *Process Biochemistry* **39**: 2183-2191.

Shackelford JF, Alexander W. 2000. CRC materials science and engineering handbook. Third edition. CRC Press, Boca Raton, Florida.

Sharma G. Jeevanandam P. 2013. A facile synthesis of multifunctional iron oxide@Ag core-shell nanoparticles and their catalytic applications. *European Journal of Inorganic Chemistry* **36**: 6126-6136.

Tang Lin, Yang GD, Zeng GM, Cai Y, Li SS, Zhou YY, Pang Y, Liu YY, Zhou Yi, Luna B. 2014. Synergistic effect of iron doped ordered mesoporous carbon on adsorption-coupled reduction of hexavalent chromium and the relative mechanism study. *Chemical Engineering Journal* **239**: 114–122.

Wang G. Xing W. Zhuo S. 2009. Application of mesoporous carbon to counter electrode for dye-sensitized solar cells. *Journal of Power Sources* **194**: 568-573.

Xin W, Song Y. 2015. Mesoporous carbons: recent advances in synthesis and typical applications. *RSC Advances* **5**: 83239-83285.

Yang G, Tang L, Cai Y, Zeng G, Guo P, Chen G, Zhou Y, Tang J, Chen J, Xiong W. 2014. Effective removal of Cr(VI) through adsorption and reduction by magnetic mesoporous carbon incorporated with polyaniline. *RSC Advances* **4**: 58362–58371.

Yang G, Tang L, Zeng G, Cai Y, Tang J, Pang Y, Zhou Y, Liu Y, Wang J, Zhang S,, Xiong W. 2015. Simultaneous removal of lead and phenol contamination from water by nitrogen-functionalized magnetic ordered mesoporous carbon. *Chemical Engineering Journal* **259**: 854–864.

Yazdankhah A, Moradi SE, Amormahmoodi S, Abbasian M, Shoja SE. 2010. Enhanced sorption of cadmium ion on highly ordered nanoporous carbon by

using different surfactant modification. *Microporous and Mesoporous Materials* **133**: 45–53.

Zeng G, Liu Y, Tang L, Yang G, Pang Y, Zhang Y, Zhou Y, Li Z, Li M, Lai M, He Z, He Y. 2015. Enhancement of Cd(II) adsorption by polyacrylic acid modified magnetic mesoporous carbon. *Chemical Engineering Journal* **259**: 153–160.

Zhang M. 2011. Adsorption study of Pb(II), Cu(II) and Zn(II) from simulated acid mine drainage using dairy manure compost. *Chemical Engineering Journal* **172**: 361-368.

Zhao D. Huo Q. Feng J. Chmelka BF. Stucky GD. 1998. Nonionic triblock and star diblock copolymer and oligomeric surfactant syntheses of highly ordered, hydrothermally stable, mesoporous silica structures. *Journal of American Chemical Society* **120**: 6024-6036.

Zhu J, Liao L, Bian X, Kong J, Yang P, Liu B. 2012. pH-controlled delivery of doxorubicin to cancer cells, based on small mesoporous carbon nanospheres. *Small* **8**: 2715-2720.

Zolfaghari G, Esmalli-Sari A, Anbia M, Younesi H, Amirmahmoodi S, Ghafari-Nazari A. 2011. Taguchi optimization approach for Pb(II) and Hg(II) removal from aqueous solutions using modified mesoporous carbon. *Journal of Hazardous Materials* **192**: 1046– 1055.

국문 초록

본 연구에서는 자성 산화 메조포러스 카본을 이용하여 수용액 상의 구리를 흡착 제거하고 이를 다시 회수하고자 하였다. 메조포러스 카본은 주형의 역할을 하는 메조포러스 실리카를 탄소 원료 물질과 고온에서 반응시킨 후 강염기로 실리카를 제거하여 합성하였으며, 이를 다시 농질산과 반응시켜 표면을 산화시킴으로써 산화철과의 친화력을 상승시키고자 하였다. 마지막으로 산화 메조포러스 카본과 산화철을 반응시킨 후 열처리하여 자성 산화 메조포러스 카본을 합성하였다.

투과전자현미경 (TEM)을 통해 자성 산화 메조포러스 카본 표면에 나노 사이즈의 기공이 형성되었음을 확인하였다. 또한 에너지 분산 분광기 (EDS) 패턴을 통해 자성 산화 메조포러스 카본의 주요 구성 원소가 탄소, 산소, 철임을 확인하였고, X 선 회절 분석기 (XRD)를 이용하여 무정형의 탄소체 피크와 마그헤마이트 또는 마그네타이트의 피크를 확인하였다. 한편 FT-IR 분광광도계를 이용하여 개질을 통해 자성 산화 메조포러스 카본의 입자 표면에 카르복실기와 Fe-O 결합이 형성된 것을 확인하였으며, 개질 전의 비표면적 값 1488.1 m^2/g 은 표면 산화와 산화철의 첨착을 거치면서 179.19 m^2/g 으로 감소하였다.

자성 산화 메조포러스 카본을 이용한 구리 제거 특성을 평가하기 위해 회분 실험을 수행하였다. 먼저 메조포러스 카본의 개질 여부에 따른 구리 이온 흡착능 변화를 관찰해 본 결과, 1 g/L 의 adsorbent

dosage 조건에서 개질 전에는 3.70 mg/g 의 흡착능을 보인 한편 표면 산화 후에는 31.89 mg/g, 최종적으로 자성을 부여한 후에는 34.89 mg/g 으로 상승하는 것으로 나타났다. 반응 시간에 따른 영향을 확인하기 위해 동역학적 실험을 수행한 결과, 자성 산화 메조포러스 카본과 구리 이온의 흡착 반응은 약 3 시간 후에 평형에 도달하는 것으로 나타났으며 Pseudo-first-order model 로 가장 잘 모사되는 것을 확인할 수 있었다. 구리 이온의 초기 농도 변화에 따른 평형 실험을 수행한 결과 Freundlich isotherm model 이 자성 산화 메조포러스 카본과 구리 이온의 흡착 메커니즘을 가장 잘 설명하는 것으로 나타났으며, 최대 흡착능 M-O-MC 의 용량이 1 g/L 인 조건에서 48.354 mg/g 으로 계산되었다. 온도에 의한 영향을 확인하기 위해 회분 실험을 수행한 결과, 온도가 상승할수록 흡착능이 증가하여 구리 이온의 자성 산화 메조포러스 카본에 대한 흡착은 흡열 반응인 것으로 확인되었다.

한편 용액 조성에 의한 자성 산화 메조포러스 카본의 구리 흡착 특성 변화를 살펴보기 위한 회분 실험을 수행하였다. 먼저 용액의 pH 에 따른 영향을 관찰해본 결과, 용액의 초기 pH 가 5 일 때 자성 산화 메조포러스 카본에 의한 구리 이온의 흡착능이 가장 높게 나타났으며, pH 가 강한 산성 조건으로 변할수록 수소 이온과의 경쟁 효과에 의해 흡착능이 감소하여 pH 가 2 인 경우에는 1.12 mg/g 의 낮은 흡착능을 보였다. 염에 의한 이온 강도가 미치는 영향을 관찰한 결과 KCl, NH_4Cl, NaCl, $CaCl_2$ 의 존재 하에 각각의 양이온과의 경쟁 효과에 의해 자성 산화 메조포러스 카본에 대한

구리 이온의 흡착능이 감소하는 것으로 나타났다. 다른 중금속과의 경쟁적인 흡착 특성을 살펴보기 위해 구리와 경쟁 중금속을 1:1 의 농도로 섞은 수용액에 대해 회분 실험을 수행한 결과 니켈, 아연, 코발트에 비하여 구리가 자성 산화 메조포러스 카본과 보다 높은 친화도를 나타내는 것으로 확인되었다.

자성 산화 메조포러스 카본에 흡착된 구리 이온은 HCl 을 용매로 하였을 때 가장 높은 탈착율을 보였다. 이를 이용하여 자성 산화 메조포러스 카본의 재이용 실험을 수행한 결과, 첫 번째 재이용 시 흡착능이 절반 이하로 감소하였으나 2 번의 추가적인 재이용 후에는 흡착능이 거의 유지되었다. 한편 구리 이온의 탈착과 동시에 M-O-MC 로부터 침출된 철 이온을 분리 회수하기 위하여 용액의 pH 를 단계적으로 상승시킨 결과 pH 5 를 기준으로 철의 침전이 완료되었으며, 이를 다시 pH 6 이상으로 상승시켜 구리를 침전시킴으로써 선택적으로 회수할 수 있었다.

본 연구를 통해서 자성 산화 메조포러스 카본을 이용한 수중 구리 이온 흡착 제거 및 회수 적용 가능성을 확인하였다.

주요어: 메조포러스 카본, 자성 산화 메조포러스 카본, 구리, 흡착, 회수, 침전

학번: 2014-20057